Journal of Medicinal Chemistry

Article

pubs.acs.org/jmc

Substituted 4-(Thiazol-5-yl)-2-(phenylamino)pyrimidines Are Highly Active CDK9 Inhibitors: Synthesis, X-ray Crystal Structures, Structure–Activity Relationship, and Anticancer Activities

Hao Shao,[†] Shenhua Shi,[†] Shiliang Huang,[†] Alison J. Hole,[§] Abdullahi Y. Abbas,[†] Sonja Baumli,[§] Xiangrui Liu,[†] Frankie Lam,[†,‡] David W. Foley,[†] Peter M. Fischer,[†] Martin Noble,[§,∥] Jane A. Endicott,[§,∥] Chris Pepper,[⊥] and Shudong Wang*[,†,‡]

[†]School of Pharmacy and Centre for Biomolecular Sciences, University of Nottingham, University Park, Nottingham NG7 2RD, U.K.

[‡]Shool of Pharmacy and Medical Sciences, University of South Australia, Adelaide, SA 5001, Australia

[§]Department of Biochemistry, University of Oxford, Oxford OX1 3QU, U.K.

[∥]Northern Institute for Cancer Research, Medical School, Newcastle University, Newcastle upon Tyne NE2 4HH, U.K.

[⊥]Institute of Cancer and Genetics, School of Medicine, Cardiff University, Heath Park, Cardiff CF14 4XN, U.K.

Supporting Information

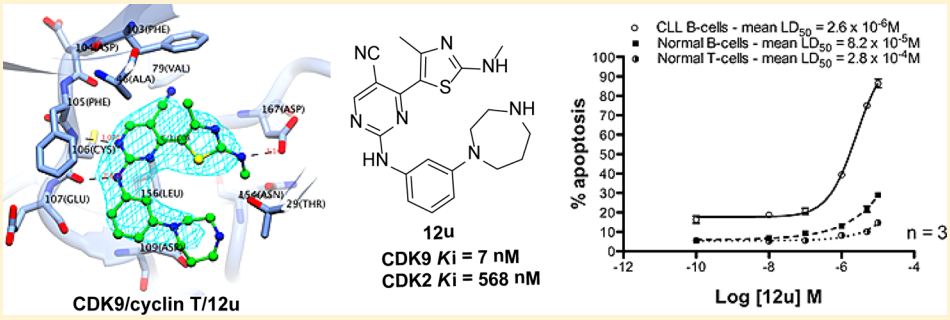

ABSTRACT: Cancer cells often have a high demand for antiapoptotic proteins in order to resist programmed cell death. CDK9 inhibition selectively targets survival proteins and reinstates apoptosis in cancer cells. We designed a series of 4-thiazol-2-anilinopyrimidine derivatives with functional groups attached to the C5-position of the pyrimidine or to the C4-thiazol moiety and investigated their effects on CDK9 potency and selectivity. One of the most selective compounds, **12u** inhibits CDK9 with IC_{50} = 7 nM and shows over 80-fold selectivity for CDK9 versus CDK2. X-ray crystal structures of **12u** bound to CDK9 and CDK2 provide insights into the binding modes. This work, together with crystal structures of selected inhibitors in complex with both enzymes described in a companion paper,[34] provides a rationale for the observed SAR. **12u** demonstrates potent anticancer activity against primary chronic lymphocytic leukemia cells with a therapeutic window 31- and 107-fold over those of normal B- and T-cells.

INTRODUCTION

Cyclin-dependent kinases (CDKs) can generally be classified into two main groups based on whether their primary role is in the control of cell cycle progression or regulation of transcription. Multiple CDKs control the cell cycle and are considered essential for normal proliferation, development, and homeostasis. CDK4/cyclin D, CDK6/cyclin D, and CDK2/cyclin E facilitate the G1-S phase transition by sequentially phosphorylating the retinoblastoma protein (Rb), while CDK1/, CDK2/cyclin A, and CDK1/cyclin B are essential for S-phase progression and G2-M transition, respectively.[1]

Most CDK inhibitors have been developed as potential cancer therapeutics based on the premise that they might counteract the uncontrolled proliferation of cancer cells by targeting the cell-cycle regulatory functions of CDKs. However in recent years, this understanding of the cellular functions and regulatory roles of CDKs has been challenged.[2,3] The observations that cancer cell lines and some embryonic fibroblasts lacking CDK2 proliferate normally and that CDK2 knockout mice are viable[4,5] suggest that this CDK performs a nonessential role in cell-cycle control. Furthermore, redundancy of CDK4 and CDK6 was also suggested in cells that enter the cell cycle normally.[6] It has been demonstrated that mouse embryos deficient in CDKs 2, 3, 4, and 6 develop to mid-gestation, as CDK1 can form complexes with their cognate cyclins and subsequently phosphorylate Rb protein. Inactivation of Rb in turn activates E2F-mediated transcription of proliferation factors.[7] In cells depleted of CDK1/cyclin B, CDK2/cyclin B is readily detectable and can facilitate G2/M

Received: October 11, 2012
Published: January 9, 2013

progression.[3] These studies suggest that specifically targeting individual cell-cycle CDKs may not be an optimal therapeutic approach because of a high level of functional redundancy and compensatory mechanisms.

By contrast, the hypothesis that inhibition of transcriptional CDKs might be an effective anticancer strategy has gained considerable support following the observation that many cells rely on the production of short-lived mitotic regulatory kinases and apoptosis regulators such as Mcl-1 for their survival.[2,8] The transcriptional CDKs, particularly CDK9/cyclin T and CDK7/cyclin H, are involved in the regulation of RNA transcription. CDK7/cyclin H is a component of transcription factor IIH (TFIIH) that phosphorylates the serine-5 residues within the heptad repeats of RNA polymerase II (RNAPII) C-terminal domain (CTD) to initiate transcription.[9,10] CDK9/cyclin T, the catalytic subunit of positive transcription elongation factor P-TEFb,[11,12] phosphorylates two elongation repressors, i.e., the DRB-sensitive-inducing factor (DSIF) and the negative elongation factor (NELF), and position serine-2 of the CTD heptad repeat to facilitate productive transcription elongation.[2,13] While CDK7 is also recognized as a CDK-activating kinase (CAK),[10] CDK9 appears to have a minimal effect on cell-cycle regulation.[14]

During the past decade an intensive search for pharmacological CDK inhibitors has led to the development of several clinical candidates and to the realization that inhibition of the transcriptional CDKs underlies their antitumor activity.[2,15] Flavopiridol (alvocidib), the first CDK inhibitor to enter clinical trials, is the most potent CDK9 inhibitor identified to date and has demonstrated marked antitumor activity in chronic lymphocytic leukemia (CLL).[16,17] Flavopiridol has been shown to inhibit multiple CDKs[18] and other kinases,[19] but the primary mechanism responsible for its observed antitumor activity in CLL appears to be the CDK9-mediated down-regulation of transcription of antiapoptotic proteins.[20,21]

R-Roscovitine (seliciclib) is the first orally bioavailable CDK inhibitor that targets CDK2, CDK7, and CDK9 ($IC_{50} \approx 0.1$, 0.5, and 0.8 μm, respectively).[22−24] During evaluation in phase I oncology monotherapy and combination chemotherapy clinical trials it was shown to be well tolerated and some evidence of disease stabilization was reported.[15] Phase II clinical trials are underway in non-small-cell lung cancer (NSCLC) patients. *R*-Roscovitine has demonstrated selective induction of apoptosis in cancer cells by down-regulation of antiapoptotic proteins through transcriptional CDK inhibition.[25,26] Other CDK inhibitors including AZD5438,[27] R547,[28,29] and AT519[30] have also been evaluated in clinical trials.

While there are several pan-CDK inhibitors in clinical studies,[27,29−31] CDK9 inhibitors with good potency and selectivity have only recently emerged.[32,33] To further exploit the sensitivity of the 4-hetertoarylpyrimidine pharmacophore (type I, Figure 1) that specifically targets the CDK9-ATP gatekeeper residue Phe103 and the ribose-binding pocket, we prepared a series of 5-substituted-2-anilino-4-(thiazol-5-yl)-pyrimidines (type II, Figure 1) and 4-(4-substituted-thiazol-5-yl)-*N*-phenylpyrimidin-2-amines (type III, Figure 1).

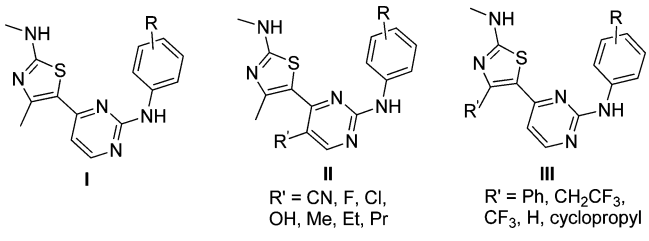

Figure 1. 4-(Thiazol-5-yl)-2-(phenylamino)pyrimidine derivatives.

Here, we report the synthesis, SAR, crystal structural analysis and biological evaluation of a novel class of 5-substituted-2-anilino-4-(thiazol-5-yl)pyrimidines and 4-(4-substituted-thiazol-5-yl)-*N*-phenylpyrimidin-2-amines. Structure−activity relationship (SAR) analysis reveals the importance of the C5-group of the pyrimidine core, in the context of a bulky substituted aniline moiety, for CDK9 potency and selectivity. A nanomolar K_i inhibitor of CDK9, **12u** demonstrates excellent selectivity with over 80-fold selectivity for CDK9 versus CDK2. This compound inhibits cellular CDK9-mediated RNA polymerase II transcription, reduces the expression level of Mcl-1 antiapoptotic protein, and subsequently triggers apoptosis in human cancer cell lines and primary CLL cells. In a companion paper[34] we also give a detailed structural analysis of several 5-substituted-2-anilino-4-(thiazol-5-yl)pyrimidines bound to CDK2 and CDK9.

CHEMISTRY

Synthesis of 2-anilino-4-thiazolpyrimidine type I compounds shown in Table 1 was carried out according to the methods described previously.[32,35] The chemistry for synthesis of 5-substituted-2-anilino-4-(thiazol-5-yl)pyrimidines (type II) is outlined in Scheme 1. Treatment of 1-methylthiourea with ethyl 2-chloro-3-oxobutanoate in pyridine resulted in ethyl 4-methyl-2-(methylamino)thiazole-5-carboxylate (**1**). The 2-methylamino group in **1** was found to interfere in subsequent reactions and was therefore masked as the *tert*-butoxycarbonate (**2**). Alkylation of **2** with cyanomethanide afforded *tert*-butyl 5-(2-cyanoacetyl)-4-methylthiazol-2-yl(methyl)carbamate (**3**, R′ = CN) in a 72% yield. Converting **3** to enaminone (**4**, R′ = CN) was achieved conveniently by refluxing in *N*,*N*-dimethylformamide−dimethylacetal (DMF−DMA).[35] **4** (R′ = CN) can also be obtained by bromination of 1-(4-methyl-2-(methylamino)thiazol-5-yl)ethanone (**5**), followed by treatment with sodium cyanide and then DMF−DMA. However, because of the requirement for highly toxic sodium cyanide, this procedure is not recommended for routine synthesis. Enaminone (**6**) was treated with SelectFluor[36,37] in methanol at 0 °C, producing 3-(dimethylamino)-2-fluoro-1-(4-methyl-2-(methylamino)thiazol-5-yl)prop-2-en-1-one (**4**, R′ = F). The analogue 2-chloro-3-(dimethylamino)-1-(4-methyl-2-(methylamino)thiazol-5-yl)prop-2-en-1-one (**4**, R′ = Cl) was obtained by treating **6** with *N*-chlorosuccinimide.[38] Preparation of alkyl-substituted enaminones (**4**, R′ = Me, Et, or Pr) started from *tert*-butyl methyl(4-methylthiazol-2-yl)carbamate (**8**), followed by treatment with alkylaldehyde (R′′CH_2CHO) in the presence of LDA to yield **9**, which was then oxidized with manganese dioxide.[39,40] Compound **8** was obtained by condensation reaction between 1-chloropropan-2-one (**7**) and 1-methylthiourea.

Reaction conditions required for preparing **4** greatly varied depending on the R′ group of the intermediates **3** and **10**. With R′ as a carbonitrile, i.e., an electron withdrawing group, **4** (R′ = CN) was conveniently obtained under mild reaction conditions. Conversely, an electron donating R′ group slowed the rate of reaction, requiring heat for an extended period of time. The enaminones (**4**, R′ = Me, Et, or *n*-propyl), for instance, were obtained under high temperature microwave conditions with low yields. The reaction became more difficult with a

dx.doi.org/10.1021/jm301475f | J. Med. Chem. 2013, 56, 640−659

Table 1. Structure and Biological Activity Summary

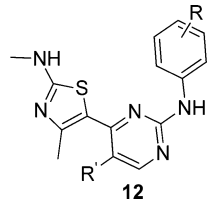

12

			kinase inhibition K_i (nM)[a]				
compd	R′	R	CDK9T1	CDK1B	CDK2A	CDK7H	cytotoxicity GI_{50} (μM),[b] HCT-116
Ia	H	*m*-NO_2	2	5	3	417	0.09
12a	CN	*m*-NO_2	6	6	1	260	0.04
12b	OH	*m*-NO_2	932	1424	>5000	>5000	3.20
Ib	H	*m*-SO_2NH_2	2	6	4	1960	0.05
12c	CN	*m*-SO_2NH_2	6	12	4	114	0.55
12d	OH	*m*-SO_2NH_2	>5000	>5000	>5000	>5000	2.03
12e	F	*m*-SO_2NH_2	4	4	3	91	<0.01
12f	Cl	*m*-SO_2NH_2	11	19	10	685	0.03
12g	Me	*m*-SO_2NH_2	5	62	34	1176	0.30
12h	Et	*m*-SO_2NH_2	98	788	845	1285	3.81
12i	Pr	*m*-SO_2NH_2	>5000	ND	>5000	ND	4.50
12j	CN	*m*-4-acetylpiperazin-1-yl	7	43	43	92	0.22
12k	CN	*m*-piperazin1-yl	5	42	56	68	0.23
12l	CN	*p*-4-acetylpiperazin-1-yl	22	45	26	316	0.82
12m	CN	*p*-piperazin-1-yl	6	79	39	71	0.03
12n	CN	*m*-piperidin-1-yl	9	35	42	286	0.93
12o	F	*m*-4-acetylpiperazin-1-yl	7	26	42	302	0.35
12p	F	*m*-piperazin-1-yl	4	24	20	193	0.31
12q	F	*m*-morpholin-4-yl	3	18	20	473	0.16
12r	Cl	*m*-piperazin-1-yl	4	88	45	155	0.26
12s	F	*m*-1,4-diazepan-1-yl	5	47	85	111	0.64
12t	CN	*m*-4-acetyl-1,4-diazepan-1-yl	7	91	131	210	0.33
12u	CN	*m*-1,4-diazepan-1-yl	7	94	568	46	0.42
Ic	H	*m*-1,4-diazepane-1-yl	19	195	320	433	0.66

[a]The ATP concentrations used in these assays were within 15 μM of K_m, i.e., 45, 45, 90, and 45 μM for CDK1/cyclin B, CDK2/cyclin A, CDK7/cyclin H/MAT1, and CDK9/cyclin T1, respectively. The data given are mean values derived from two replicates. Apparent inhibition constants (K_i) were calculated from IC_{50} values and the appropriate K_m (ATP) values for each kinase.[35] [b]Antiproliferative activity by MTT 48 h assay. The data given are mean values derived from at least three replicates.

Scheme 1. Synthesis of 3-(Dimethylamino)-2-(4-methyl-2-(methylamino)thiazole-5-carbonyl)acrylonitrile and Derivatives[a]

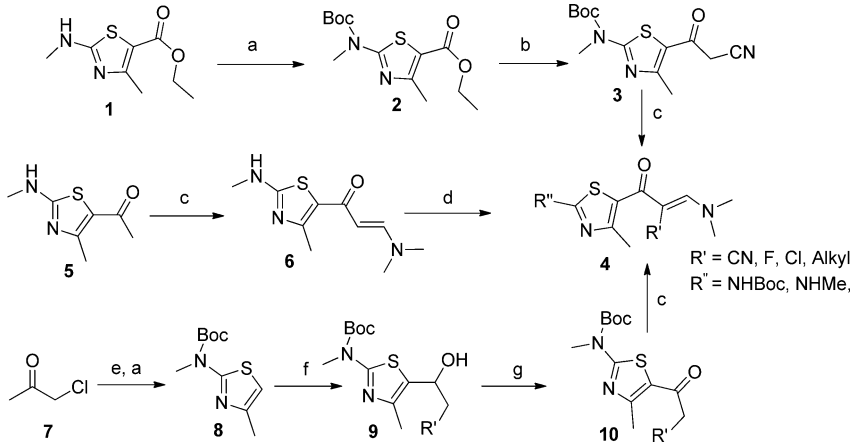

1 2 3 4 5 6 7 8 9 10

[a]Reagents and conditions: (a) di-*tert*-butyl dicarbonate, 4-dimethylaminopyridine (DMAP), DCM, rt, 1 h, 93%; (b) LDA, MeCN, THF, −78 °C, 1.5 h, 72%; (c) *N*,*N*-dimethylformamide−dimethylacetal (DMF−DMA), reflux, overnight or microwave, Δ, 20−45 min, 30−80%; (d) SelectFluor, MeOH, 0 °C, 1 h; or NCS, MeOH, rt 0.5 h, 30%; (e) 1-methylthiourea, MeOH, pyridine, rt 4 h, 88%; (f) LDA, R′CH_2CHO, MeCN, THF, −78 °C, 1−1.5 h, 53−77%; (g) MnO_2, $CHCl_3$, Δ, 3 h, 65−85%.

dx.doi.org/10.1021/jm301475f | J. Med. Chem. 2013, 56, 640−659

bulkier alkyl group; thus, attempting the synthesis of **4**, where R′ = isopropyl, failed even under harsher reaction conditions because of unfavorable electronic and steric effects of the bulky isopropyl group. Pyrimidine ring formation reaction was performed under conditions similar to those we have developed for the synthesis of 2-anilinoamino-4-(heteroaryl)pyrimidines.[35] The limiting factor in the preparation of type II analogues was the efficiency of the condensation reactions between the substituted phenylguanidines (**11**) and **4** (Scheme 2). In general, microwave-aided protocols were more effective in terms of reducing reaction times and improving yields in the pyrimidine condensation reactions compared to conventional methodology. Analogues **12b** and **12d**, where R′ = OH, were obtained from condensation of **4** (R′ = Cl) with corresponding phenylguanidines **11**, followed by in situ hydrolysis.

Scheme 2. Synthesis of 4-(4-Methylthiazol-5-yl)-2-(phenylamino)pyrimidine-5-carbonitrile and Derivatives[a]

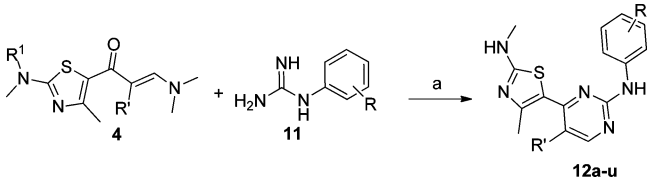

[a]Reagents and conditions: (a) 2-methoxyethanol, microwave, 200–300 W, Δ, 20–45 min.

In order to extend the SARs, we prepared another series of compounds with functional group R′ at the C4-position of the thiazol ring system (type III, Figure 1); the chemistry is outlined in Scheme 3. 2-Methylaminothiazol-5-ylethanone derivative **14** was obtained by bromination of **5** in the presence of PTSA to afford **13**, which was then treated with di-*tert*-butyl dicarbonate, followed by reaction with methyl 2,2-difluoro-2-(fluorosulfonyl)acetate in the presence of a catalytic amount of CuI.[41] Converting **14** to the corresponding enaminone **15** (R^1 = Boc, R′′ = CH_2CF_3) was achieved by reacting **14** with DMF–DMA as described above. To prepare analogue **17**, 1,1,1-trifluoropentane-2,4-dione was treated with hydroxy(tosyloxy)iodobenzene,[42] followed by reaction with 1-methylthiourea and then di-*tert*-butyl dicarbonate. *tert*-Butyl (5-acetylthiazol-2-yl)(methyl)carbamate (**20**) was obtained by cyclization reaction between chloroacetone chloride and *N*′-carbamothioyl-*N*,*N*-dimethylformimidamide (**18**),[43] giving **19**, followed by treating the latter with di-*tert*-butyl dicarbonate. To prepare *tert*-butyl(5-acetyl-4-cyclopropylthiazol-2-yl)(methyl)-carbamate (**24**), bromination of 1-cyclopropylethanone (**21**) yielded 2-bromo-1-cyclopropylethanone (**22**), which was subsequently reacted with 1-methylthiourea and then di-*tert*-butyl dicarbonate to afford 4-cyclopropyl-*N*-methylthiazol-2-amine (**23**). Acetylation was achieved by LDA-mediated alkylation reaction between **23** and acetaldehyde,[39] followed by oxidation of the resulting thiazol-5-ylethanol intermediate with MnO_2. 4-Phenylthiazol derivative (**26**) was prepared by condensation reaction between 2-chloro-1-phenylethanone and

Scheme 3. Synthesis of *N*-Methyl-5-(2-(phenylamino)pyrimidin-4-yl)-4-thiazol-2-amine Derivatives[a]

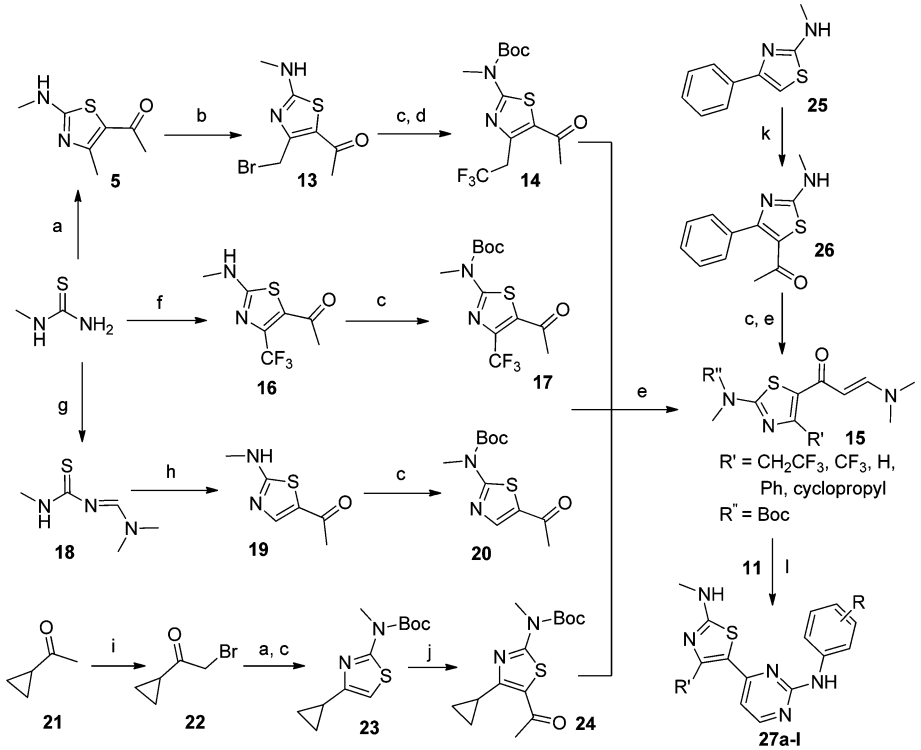

[a]Reagents and conditions: (a) pentane-2,4-dione, pyridine, EtOH, rt 4 h; (b) NBS, *p*-tolenensulfonic acid (PTSA), $CHCl_3$, 0–5 °C, 1 h, 56%; (c) di-*tert*-butyl dicarbonate, DMAP, DCM, rt 2 h; (d) methyl 2,2-difluoro-2-(fluorosulfonyl)acetate, CuI, DMF, Δ, 12 h; (e) DMF–DMA, Δ, overnight, or microwave, Δ, 45 min; (f) (i) 1,1,1-trifluoropentane-2,4-dione, hydroxy(tosyloxy)iodobenzene, MeCN, Δ, 1 h; (ii) 1-methylthiourea, Δ, 4 h, 53%; (g) DMF–DMA, $CHCl_3$, Δ, overnight, 98%; (h) chloroacetone chloride, MeCN, Δ, 4 h, 79%; (i) Br_2, 0 °C to rt 4 h, 77%; (j) (i) LDA, acetaldehyde, THF, −78 °C, 2 h, 49%; (ii) MnO_2, $CHCl_3$, Δ, 4 h, 55%; (k) acetyl chloride/$AlCl_3$, rt, 2 h, 67%; (l) **11**, 2-methoxyethanol, microwave 200–300 W, Δ, 20–45 min.

dx.doi.org/10.1021/jm301475f | J. Med. Chem. 2013, 56, 640–659

1-methylthiourea to afford *N*-methyl-4-phenylthiazol-2-amine, followed by the Friedel−Crafts acylation reaction. Finally, the enaminones (**15**) were converted to the corresponding pyrimidines (**27a−l**) upon treatment with the appropriate phenylguanidines[32,35] under microwave irradiation conditions.

RESULTS AND DISCUSSION

Inhibitor Design and SAR Analysis. We previously identified a series of 2-herteroaryl-4-anilinopyrimidine CDK inhibitors.[32,35,44] Many of these compounds showed potent CDK9 inhibitory activity. The lead compounds demonstrated excellent pharmaceutical properties and in vivo antitumor efficacy.[32] However, CDK9 specificity was not achieved, as they cross-reacted with other cell cycle CDKs, in particular CDK2.

Previously established SARs of 2-anilino-4-(thiazol-5-yl)-pyrimidines (type I, Figure 1) with respect to CDK2 suggested the importance of substituents at the C2-position in the thiazole ring.[32,35] It was found that introduction of amino functions, in the context of either meta- or para-substituted anilines at the C2-pyrimidine ring, resulted in a significant increase of inhibitory activity not only against CDK2 but also against CDK9. Cocrystal structures of some of these inhibitors bound to CDK2 revealed that the thiazole C2-amino group interacted strongly with the Asp145 residue of CDK2, enhancing the hydrophobic interactions of the thiazol C4-methyl group with the Phe80 gatekeeper residue of CDK2 (Phe103 in CDK9). Additional hydrogen bonding interactions between the thiazole C2-amino groups and Gln131 and Asp86 of CDK2 were also observed. Substitution of the thiazole C2-amino group with a C2-methylamino or C2-ethylamino appeared to have a detrimental effect on CDK2 and CDK4 activity while having only a minimal effect on CDK9 potency.[32,35] A bulkier group, such as phenyl, pyridyl, or other heterocycles at this position, however, led to significantly reduced activity against all CDKs. We therefore designed a series of 5-substituted-4-thiazolpyrimidines in the context of the C2-methylamino to improve potency and selectivity against CDK9.

The SAR analysis of the pyrimidinyl C2-aniline moiety was previously described.[32,35] It was shown that many meta- or para-substitutions of the aniline, in the context of the 4-thiazolpyrimidine, were well tolerated and manipulation of these substituents led to a number of inhibitors possessing varying CDK selectivity profiles. In many cases, meta-substituted anilines gave rise to selectivity for CDK9 over CDK2 compared with their para-substituted aniline analogues. However, substituents in the ortho position abolished CDK-inhibitory activity in all cases.

It is recognized that the ATP-binding sites are highly conserved among kinases,[45] but the nonconserved hydrophobic region, which is not occupied by ATP, and the so-called "gatekeeper" region can be exploited for inhibitor design.[4647−50]A cocrystal structure of flavopiridol bound to CDK9 showed that the hydrophobic region that accommodates the chlorophenyl ring of flavopiridol is more open in CDK9 than CDK2. CDK9 Gly112 takes the place of CDK2 Lys89 and creates a less crowded and a different electrostatic environment.[51] Analysis of the previously published 2-anilino-4-(thiazol-5-yl)pyrimidine CDK2-bound crystal structures and their corresponding models of CDK9 binding[32,35] suggested that an appropriate functional group at either the C5-pyrimidine or the C4-thiazol moiety might enhance interactions with the CDK9 gatekeeper region. We thus investigated the potency and selectivity of a series of 5-substituted 2-anilino-4-(thiazol-5-yl)-pyrimidines against CDKs and characterized their cellular antitumor activity. The results are summarized in Table 1.

Compound **Ia** (R′ = H, R = *m*-NO_2) is a highly potent pan-CDK inhibitor. Substitution of hydrogen at C5-pyrimidine in **Ia** with a carbonitrile group results in compound **12a** (R′ = CN, R = *m*-NO_2) that exhibits a similar potency and selectivity profile. Both compounds inhibit CDK9, CDK1, and CDK2 potently with K_i values ranging from 1 to 6 nM but are significantly less active toward CDK7. Both compounds are highly effective antiproliferative agents with respective GI_{50} values of 90 and 40 nM in the HCT-116 human colon cancer cell line. Replacement of the C5-carbonitrile with a C5-hydroxyl group in **12b** (R′ = OH, R = *m*-NO_2) results in over 155-fold and 230-fold loss in CDK9 and CDK1 inhibition, respectively. This replacement also abolishes CDK2 and CDK7 inhibitory activity and significantly reduces cellular antiproliferative activity. A compound containing the *m*-sulfonamideaniline ring, **12c** (R′ = CN, R = *m*-SO_2NH_2), shows similar potencies against CDK1, CDK2, and CDK9 but a 17-fold or a 10-fold loss in CDK7 inhibition and cellular toxicity, respectively, compared to **Ib** (R′ = H, R = *m*-SO_2NH_2). Again, introducing a hydroxyl group at C5-pyrimidine, in the context of *m*-sulfonamideaniline, is not tolerated; **12d** (R′ = OH, R = *m*-SO_2NH_2) shows little biological activity in the enzymatic and cellular assays. These results demonstrate the importance of C5-substitution of the pyrimidine and that a protic or hydrogen bond donating function at this position has a detrimental effect on biological activity. Compound **12e** (R′ = F, R = *m*-SO_2NH_2), a potent pan-CDK inhibitor (K_i = 3−7 nM), is the most potent antiproliferative agent of this series, with GI_{50} < 10 nM against HCT-116 cells. Analogue **12f**, where R′ = Cl, R = *m*-SO_2NH_2, however, displays a >3-fold reduced CDK inhibitory activity and cellular potency compared to **12e**. A more interesting trend toward CDK9 selectivity is observed with C5-alkylpyrimidines; **12g** (R′ = Me, R = *m*-SO_2NH_2) exhibits a CDK9 inhibitory potency similar to that of **12e** with K_i = 5 nM but enhances selectivity for CDK9 with >7-fold lower effectiveness against other CDKs. However, this selectivity results in **12g** showing over 30-fold reduced cytotoxicity in HCT-116 cells compared to **12e**. With further introduction of a bulkier alkyl group, CDK9 inhibitory activity dramatically decreases; thus, **12h** (R′ = Et, R = *m*-SO_2NH_2) is 20-fold less potent against CDK9 than **12g**, while **12i** (R′ = Pr, R = *m*-SO_2NH_2) is not active against CDKs at concentrations up to 5 μM. As expected, **12h** and **12i** are also less cytotoxic in cancer cells with respective GI_{50} values of 3.81 and 4.50 μM.

Retaining the C5-carbonitrile pyrimidine core but replacing the *m*-sulfonamide with a bulkier 1-(piperazin-1-yl)ethanone or piperazine leads to the corresponding **12j** (R′ = CN, R = *m*-1-(piperazin-1-yl)ethanone) or **12k** (R′ = CN, R = *m*-piperazine). This not only maintains CDK9 potency but also increases selectivity (∼10-fold) over CDK2 compared to **12c**, indicating the tolerance of a large ring system in the corresponding CDK9 binding region. Compounds **12m−r**, bearing heterocyclic piperidine, 1-(piperazin-1-yl)ethanone, piperazine, or morpholine at the meta- or para-position of the aniline in the context of a C5-carbonitrile or C5-halogen pyrimidine moiety, display favorable CDK9 inhibitory activity with low nanomolar potencies and possesses over 4-fold selectivity for CDK9. The exception is compound **12l** (R′ = CN, R = *p*-1-(piperazin-1-yl)ethanone), which shows a >3-fold loss of potency against

dx.doi.org/10.1021/jm301475f | J. Med. Chem. 2013, 56, 640−659

Table 2. Structure and Biological Activity Summary

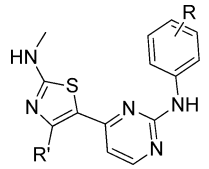

27a-l

			kinase inhibition K_i (nM)[a]				
compd	R′	R	CDK9T1	CDK1B	CDK2A	CDK7H	cytotoxicity GI_{50} (μM),[b] HCT-116
27a	Ph	*m*-NO_2	>5000	>5000	>5000	>5000	0.06
27b	CH_2CF_3	*m*-NO_2	134	>5000	>5000	>5000	0.90
27c	CH_2CF_3	*m*-OH	245	556	282	3474	2.60
27d	CH_2CF_3	*p*-OH	278	334	347	1543	3.70
27e	CH_2CF_3	*m*-SO_2NH_2	156	154	226	1984	0.91
27f	CF_3	*m*-SO_2NH_2	2	1.5	2	47	0.05
27g	CF_3	*p*-SO_2NH_2	3	0.5	1.5	64	0.01
27h	H	*p*-SO_2NH_2	5	1	1	54	0.13
27i	H	*m*-SO_2NH_2	3	4	5	40	0.02
27j	cyclopropyl	*m*-SO_2NH_2	16	18	2	273	0.41
27k	cyclopropyl	*p*-SO_2NH_2	8	2	13	255	0.08
27l	cyclopropyl	*m*-1,4-diazepan-1-yl	66	176	326	464	0.77

[a]The ATP concentrations used in these assays were within 15 μM of K_m. The data given are mean values derived from two replicates. Apparent inhibition constants (K_i) were calculated from IC_{50} values and the appropriate K_m (ATP) values for each kinase.[35] [b]Antiproliferative activity by MTT 48 h assay. The data given are mean values derived from at least three replicates.

CDK9. All these analogues demonstrate excellent antiproliferative activity with GI_{50} values ranging from 0.03 to 0.93 μM.

Introduction of a bulkier heterocylic (1,4-diazepan-1-yl)-ethanone or 1,4-diazepane at the meta-position of the aniline affords **12s−u**, displaying appreciable selectivity for CDK9 versus CDK2. Compound **12u**, in particular, shows a >80-fold enhanced CDK9 selectivity over CDK2. Compounds **12s−u** effectively inhibit tumor cell growth with GI_{50} values of 0.64, 0.33, and 0.42 μM, respectively. Replacement of the C5-carbonitrile or C5-fluoride with a C5-hydrogen affords **Ic** (R′ = H, R = *m* -1,4-diazepane). However, this replacement results in a >2-fold loss in CDK9 inhibitory activity but a more significant drop in CDK2 selectivity when compared with **12s** and **12u**. These further support the role of the carbonitrile or fluoride substitution at the C5-pyrimidine in favoring potency and selectivity against CDK9 over CDK2.

In general, all C5-substituted pyrimidine analogues are also potent CDK1 inhibitors, with activity comparable to that of CDK2 as shown in Table 1. An exception is compound **12u** which targets CDK1 and CDK2 with K_i values of 94 and 568 nM, respectively, being 6-fold more potent for CDK1 than for CDK2. It is apparent that this combined inhibition of CDK9, CDK1, and CDK2 results in significant cytotoxicity in cancer cells. **12e**, a nanomolar CDK9, CDK1, and CDK2 inhibitor, for example, is the most potent cytotoxic agent of this chemical class, with GI_{50} < 10 nM against HCT-116 cells. This is consistent with the finding that cancer cells expressing shRNA targeting a combination of CDK2, CDK1, and CDK9 were most effective in induction of apoptosis of cancer cells, and targeting CDK9, CDK1, and CDK2 has been proposed as an anticancer strategy.[3]

Most of the analogues described here are significantly less effective as CDK7 inhibitors when compared to their activity against other CDKs, suggesting that CDK7 inhibition is not a requirement for the observed cellular cytotoxicity: many compounds demonstrate excellent antiproliferative activity irrespective of modest CDK7 inhibition (Table 1). Compounds **Ib** and **12g**, for example, inhibit CDK7 with K_i > 1 μM, but both exhibit excellent antiproliferative activity with GI_{50} = 0.05 and 0.30 μM, respectively.

In order to assess whether modification of the C4-methyl of the thiazole is tolerated, we prepared a series of substituted C4-thiazolpyrimidine derivatives; the SAR is summarized in Table 2. Replacement of the C4-methyl with phenyl (**27a**, R′ = Ph, R = *m*-NO_2) is not tolerated, and no inhibitory activity against CDKs is detected up to 5 μM. However, this compound exhibits potent antiproliferative activity with a GI_{50} of 60 nM, indicating potential non-CDK kinase targets. Substitution of C4-trifluoroethyl, in the context of *m*-nitroanilinopyrimidine, yields **27b** (R′ = CH_2CF_3, R = *m*-NO_2). This compound exhibits excellent selectivity for CDK9 (K_i = 0.134 μM), being inactive against other CDKs at concentrations up to 5 μM. Despite its high selectivity, **27b** still displays good antiproliferative activity with GI_{50} < 1 μM in HCT-116 cancer cells. However, analogues **27c** (R′ = CH_2CF_3, R = *m*-OH), **27d** (R′ = CH_2CF_3, R = *p*-OH), and **27e** (R′ = CH_2CF_3, R = *m*-SO_2NH_2) reduce CDK9 inhibition and selectivity when compared to **27b**. Keeping the benzenesulfonamide moiety but replacing the 4C-trifluoroethyl with a C4-trifluoromethyl, C4-hydrogen, or C4-cyclopropyl affords compounds **27f−k**. All of these compounds possess significantly enhanced inhibitory activity not only against CDK9 but also against other CDKs. As expected, these compounds are extremely cytotoxic to cancer cells with GI_{50} values in the range of 0.01−0.41 μM. However, substitution of the benzenesulfonamide with 1,4-diazepan-1-ylaniline yields **27l** (R′ = cyclopropyl, R = *m*-1,4-diazepane). This analogue shows a significant loss of activity which suggests that the benzenesulfonamide moiety is a key contributor to optimal CDK inhibition and cellular potency of this series.

Cocrystal Structures of 12u Bound to CDK9/Cyclin T and CDK2/Cyclin A. As one of the most selective CDK9 inhibitors in the chemical series, **12u** was cocrystallized with

dx.doi.org/10.1021/jm301475f | J. Med. Chem. 2013, 56, 640−659

Table 3. Crystallographic Parameters of CDK2/Cyclin A/12u and CDK9/Cyclin T/12u

	CDK2/cyclin A/**12u**	CDK9/cyclin T/**12u**
Data Collection		
beamline	Diamond I-03	Diamond I-03
space group	$P2_12_12_1$	$H3$
unit cell (Å)	a = 73.81; b = 134.55; c = 149.17	$a = b$ = 172.80; c = 98.88
unit cell (deg)	$\alpha = \beta = \gamma$ = 90	$\alpha = \beta$ = 90; γ = 120
resolution (highest resolution shell) (Å)	29.83−2.26 (2.38−2.26)	86.40−3.08 (3.25−3.08)
total observations	308028 (43211)	70331 (10036)
unique observations	69656 (9807)	20079 (2956)
R_{merge}	0.071 (0.496)	0.058 (0.511)
multiplicity	4.4 (4.4)	3.5 (3.4)
mean I/σ_I	13.4 (2.8)	15.4 (2.4)
completeness (%)	99.2 (96.6)	99.0 (99.6)
Refinement Statistics		
highest resolution shell (Å)	2.29−2.26	3.09−3.17
total number of atoms	9233	4649
total number of waters	363	16
R	18.10 (23.09)	16.11 (28.6)
R_{free}	21.71 (28.66)	19.72 (34.2)
rms bonds (Å)	0.003	0.011
rms angles (deg)	0.702	1.433

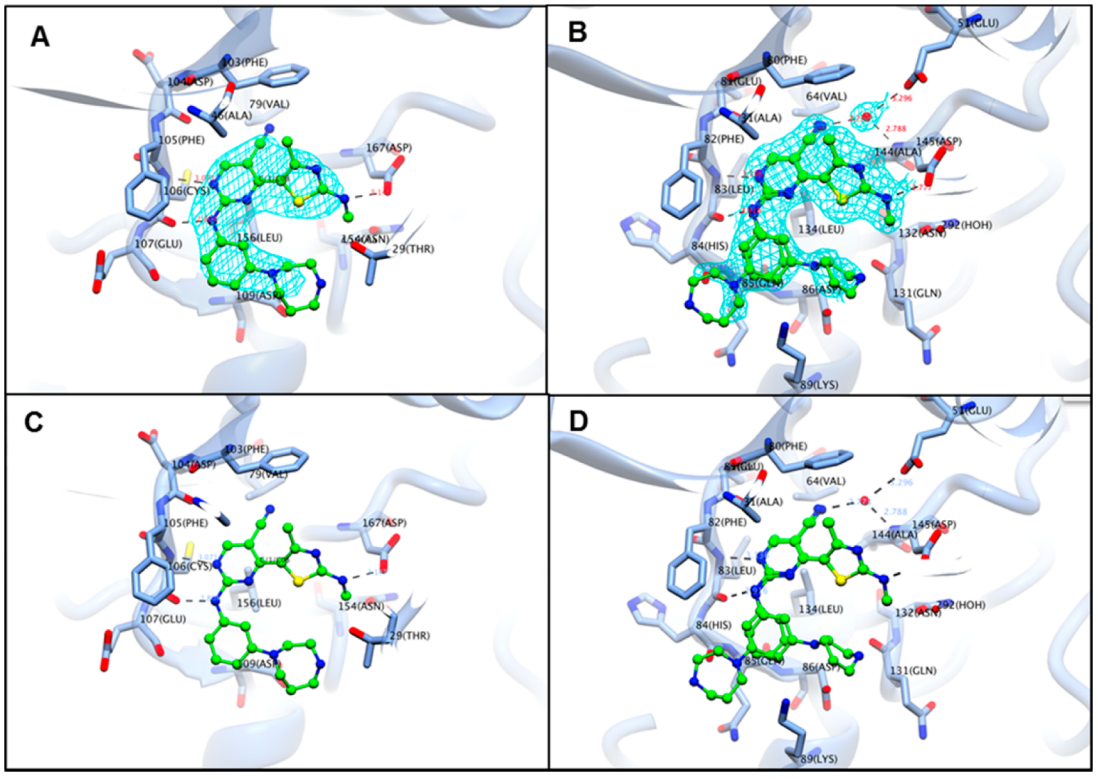

Figure 2. Cocrystal structures of **12u** bound to CDK9/cyclin T1 (PDB code 4BCG) and CDK2/cylin A (PDB code 4BCP). The structures of CDK9/T1/**12u** (A, C) are shown. Compound **12u** bound to CDK2/cyclin A (B, D) and showing two binding orientations. Electron density around **12u** is shown as a wire mesh (A, B). Selected CDK9 and CDK2 residues are drawn in ball-and-stick representation. Hydrogen bonds in all panels are depicted by dotted lines.

CDK9/cyclin T and CDK2/cyclin A in order to explain the observed SAR. The crystal structure and refinement data are summarized in Table 3. A more thorough rationalization of the SARs provided by the determination of five additional inhibitor cocrystal structures bound to CDK9/cyclin T and CDK2/cyclin A is provided in the companion paper.[34] As shown in Figure 2, **12u** adopts a similar binding mode within the CDK9 and CDK2 ATP binding sites located between the N- and C-terminal lobe, and the thiazole, pyrimidine, and aniline moieties occupy similar positions. In both CDK9 and CDK2, **12u** hydrogen-bonds with the kinase hinge regions. The N1-pyrimidine accepts a hydrogen bond from the peptide nitrogen of Cys106 (Leu83 in CDK2), while the C2-NH of the pyrimidine ring donates a hydrogen bond to the peptide

dx.doi.org/10.1021/jm301475f | J. Med. Chem. 2013, 56, 640−659

carbonyl of Cys106. At the back of the ATP binding site the C5-carbonitrile group exploits the hydrophobic region close to the gatekeeper residue Phe103 (Phe80 in CDK2) to form a favorable lone pair−π interaction. The CDK2/cyclin A/**12u** structure was determined at a higher resolution and shows a water molecule trapped in a pocket behind the C5-carbonitrile (Figure 2B and Figure 2D). This water molecule forms a hydrogen-bond network with the backbone of residue Asp145 and with the side chain of Glu51. In the adenine site the pyrimidine ring is sandwiched between the hydrophobic side chains of Ala46 (Ala31 in CDK2) and Leu156 (Leu134 in CDK2), with which it forms extensive van der Waals interactions. The hydrogen of the C2-methylaminothiazole binds to Asp167 in CDK9 and to the corresponding residue Asp145 in CDK2. At the front of the ATP binding pocket, the aniline ring is contacted from above by Ile25 (Ile10 in CDK2) to make favorable van der Waals interactions with both enzymes.

The very weak electron density of the 1,4-diazepan-1-ylaniline moiety of **12u** suggests that it is not bound tightly to CDK2. Two conformations of **12u** were consistent with the observed electron density and represent possible alternative binding modes. Neither of these modes suggests either favorable or unfavorable interactions, correlating to the relative absence of electron density for the 1,4-diazepane ring. In the CDK9 complex, however, the 1,4-diazepane ring clearly adopts an "inward" conformation orientated toward the thiazole ring. This may be more favorable for **12u** because of a reduced solvent exposure of the hydrophobic 1,4-diazepane ring in this orientation.

Although the inhibitor interactions with CDK2 and CDK9 are mostly conserved, there are, however, two significant differences. First, as seen for other CDK9/cyclin T inhibitor structures described in the companion paper,[34] the binding of the inhibitor induces a lowering of the glycine-rich loop into the ATP binding site. The loop adopts several conformations, and this inherent flexibility is reflected in the higher *b*-factors. By contrast, the conformation of the glycine rich loop in CDK2/cyclin A appears to be relatively unaltered on inhibitor binding (PDB 2JGZ). Second, in comparison with the apo structure of CDK9/cyclin T (PDB 3BLH)[51] the backbone of the hinge region adapts to inhibitor binding by shifting away from **12u**. This shift enables a hydrogen bond to form between the C2-NH of the pyrimidine with the peptide carbonyl of Cys106 at an optimal length of 2.8 Å. These two observations support the hypothesis that CDK9 has a more flexible ATP binding pocket than CDK2.

We propose that the greater flexibility of the ATP-binding site of CDK9 enables the large flexible anilino-1,4-diazepine of **12u**, in the context of the C5-carbonitrilepyrimidine moiety, to be well accommodated by CDK9. In contrast, the crystal structure of **12u** bound to CDK2 shows that this ring adopts an orientation either "inward" or "outward", suggesting that the CDK2 binding pocket is too crowded for **12u**. This variation in the ability of the kinases to adapt and readily accommodate inhibitors offers an explanation for the high potency and selectivity of **12u** toward CDK9.

Compound 12u Is a Potent Antiproliferative Agent. Compound **12u** was screened against a panel of kinases using biochemical assays and showed no inhibitory activity at concentrations up to 5 μM against a panel of kinases, including BCR-Abl, CaMK1, IKK, Lck, MARK2, PKA, PKB, PKC, and cSRC (Table 4). The antiproliferative effects of **12u** against a panel of nine tumor cell lines and three nontranformed cell lines were examined using a 48 h MTT assay as summarized in Table 5A. To investigate cell-type sensitivity, we included HCT-116 colon carcinoma (wild-type and mutant p53, respectively), MCF-7 breast carcinoma (wild-type p53, pRb positive, ER positive and containing CDK4/cyclin D and CDK6/cyclin D), and MDA-MB-468 breast carcinoma cells (mutant p53, pRb negative, ER negative and lacking CDK4/cyclin D and CDK6/cyclin D),[52] and other cell lines. Similar sensitivity is observed for cells with different p53, Rb, and CDK4/6 status. Compound **12u** suppresses tumor cell proliferation with GI_{50} values ranging from 0.38 to 0.78 μM, irrespective of the tumor cell type. However, all non-transformed cell lines, i.e., microvascular endothelial cell line HMEC-1 and embryonic lung fibroblasts MRC-5 and WI-38, are significantly less sensitive to **12u** treatment (GI_{50} = 3.12−5.96 μM). The time-course assays were performed using A2780 ovarian cancer and MRC-5 and HMEC-1 nontransformed cell lines. As shown in Table 5B, 24 h treatment with **12u**, as well as with flavopiridol, is sufficient to achieve maximal growth inhibition of **12u** in A2780 cancer cells. Again, **12u** is significantly less toxic in the HMEC-1 and MRC-5 non-transformed cells. In contrast, flavopiridol fails to demonstrate any significant differential effects between the cancer cells and noncancerous cell lines.

Table 4. Inhibitory Activity of 12u against Protein Kinases

protein kinases	inhibition IC_{50} (nM)[a]
CDK1/cyclin B	188
CDK2/cyclin A	1126
CDK6/cyclin D3	>5000
CDK7/cyclin H	92
CDK9/cyclin T1	14
BCR-Abl	>5000
CaMK1	>5000
IKKβ	>5000
Lck	>5000
MAPK2	>5000
PKA	>5000
PKBα	>5000
PKCα	>5000
cSRC	>5000

[a]The ATP concentrations used in these assays were within 15 μM of K_m. The data given are mean values derived from two replicates.

Compound 12u Effectively Induces Cancer Cell Apoptosis. Cell death induced by therapeutic agents can occur through caspase-dependent or -independent apoptosis or by necrosis. To assess whether apoptosis is contributing to the cytotoxic effect of **12u**, we used annexin V/PI (propidium iodide) surface staining in A2780 cancer cells following treatment with **12u** for 48 h (Figure 3A). Compound **12u** induced cell apoptosis at the GI_{50} (the concentration of **12u** required to inhibit 50% of cell proliferation by MTT assay) in a dose-dependent manner. At the GI_{50} concentration **12u** causes 38% annexin V-positive cells and the percentage increases to 50% at $5GI_{50}$. With flavopiridol the same treatments results in 39% and 54% apoptotic cells at GI_{50} and $5GI_{50}$, respectively. Concurrent treatment with $5GI_{50}$ of either **12u** or flavopiridol together with 50 μM of the pan-caspase inhibitor Z-VAD-fmk suppresses apoptosis, suggesting a caspase-dependent mechanism of apoptosis induction.[18]

dx.doi.org/10.1021/jm301475f | J. Med. Chem. 2013, 56, 640−659

Table 5. Antiproliferative Activity of 12u and Flavopiridol against a Panel of Human Humour and Nontranformed Cell Lines (A) and Activity by MTT Time-Course Experiments (B)[a]

A		
human cell line		
origin	designation	48 h MTT, GI_{50} ± SD (μM)
colon carcinoma	HCT-116 (p53wt, pRb^+)	0.420 ± 0.020
	HCT-116 (p53null)	0.780 ± 0.060
	HCC 2998 (p53wt, pRb^+)	0.385 ± 0.091
breast carcinoma	MCF-7 (p53wt, pRb^+, ER^+)	0.690 ± 0.020
	MDA-MB468 (p53mut, pRb^-, ER^-)	0.402 ± 0.026
ovarian carcinoma	A2780	0.320 ± 0.010
cervical carcinoma	HeLa	0.630 ± 0.140
renal carcinoma	TK 10	0.747 ± 0.076
pancreatic carcinoma	PANC-1	0.590 ± 0.078
microvascular endothelial	HMEC-1	3.120 ± 0.320
embryonic lung fibroblast	MRC-5	5.960 ± 0.720
	WI-38	5.490 ± 0.630

B				
		antiproliferative activity, GI_{50} ± SD (μM)		
cell line	compd	24 h	48 h	72 h
A2780	**12u**	0.493 ± 0.048	0.320 ± 0.010	0.288 ± 0.020
	flavopiridol	0.023 ± 0.001	0.031 ± 0.008	0.029 ± 0.001
MRC-5	**12u**	6.250 ± 0.515	5.960 ± 0.720	5.670 ± 0.410
	flavopiridol	0.049 ± 0.004	0.039 ± 0.012	0.028 ± 0.001
HMEC-1	**12u**	7.500 ± 1.020	3.120 ± 0.320	4.500 ± 0.310
	flavopiridol	0.061 ± 0.001	0.062 ± 0.004	0.066 ± 0.002

[a]The data given are mean values derived from at least three replicates ± SD.

Activation of caspase-3 activity by **12u** was confirmed in A2780 cancer cell following exposure to drug for 24 h and was used to compare that in HMEC-1 untransformed endothelial cells (Figure 3B). Compound **12u** significantly activates caspase-3 activity in the tumor cells starting at GI_{50} concentration ($p < 0.001$), and the effect is further enhanced at higher concentrations. In contrast, no such activity is detected in the HMEC-1 cells up to $10GI_{50}$ concentrations of **12u**. These results confirm that the cytotoxicity induced by **12u** is mediated through the preferential induction of apoptosis in cancer cell lines and corroborates the MTT cytotoxic potency.

As **12u** showed potent CDK1 inhibition in biochemical kinase assays, we next investigated its effects on cell cycle progression. A2780 cells were treated with **12u** (or flavopiridol) for a period of 24 h at GI_{50} and $5GI_{50}$ concentrations, respectively (Figure 3C). The cells showed no alteration in cell cycle distribution at concentrations less than $5GI_{50}$ **12u**, at which concentration accumulation of cells in G2/M phase of the cell cycle was detected. This confirms that **12u** has a lower cellular CDK1 inhibitory activity compared to that of CDK9. A similar cell cycle profile is observed with flavopiridol (Figure 3C).

Compound 12u Inhibits CDK9 Activity and Down-Regulates Mcl-1 in Cancer Cells. We next investigated the cellular mode of action of **12u** by Western blot analysis (Figure 3D). Treatment of A2780 cells with **12u** for a period of 24 h showed that phosphorylation at Ser-2 CTD of RNAPII was reduced at the GI_{50} and abrogated at $5GI_{50}$, confirming cellular CDK9 inhibition. The same treatment caused down-regulation of Mcl-1 and HDM2 but had little effect on the levels of Bcl-2 expression. Induction of apoptosis was indicated by PARP cleavage. Analogous results were obtained with flavopiridol, with inhibition of the phosphorylation of Ser-2 of RNAPII CTD, reduction of Mcl-1 and HDM2, and induction of cleaved PARP being observed.

Ex Vivo Antitumor Activity in Primary Chronic Lymphocytic Leukemia Cells. The potency and selectivity of **12u** were further evaluated in patient-derived CLL cells (Table 6), as well as age-matched normal B-cells and T-cells, using an annexin V-FITC apoptosis assay. As shown in Figure 4A, the compound exhibits excellent activity with a mean LD_{50} of 2.60 μM ± 1.1 μM against CLL cells (the concentration of **12u** required to kill 50% of the CLL cells following exposure for 48 h). Figure 4B shows that **12u** induces a dose-dependent increase in apoptosis in CLL cells as denoted by an increased annexin V positivity. In contrast, little toxicity is observed in the normal B- and T-cells with LD_{50} of >80 and >280 μM, respectively (Figure 4A). To determine whether the cytotoxicity induced by **12u** is caspase-dependent, primary CLL cells were incubated with various concentrations of **12u** for 24 h, followed by flow cytometric assessment of active caspase-3. As shown in Figure 4C, the caspase-3 activity is significantly induced at 1.0 μM **12u** ($P < 0.05$) and is further enhanced in a dose-dependent manner at 5 μM ($P < 0.0001$) and 10 μM ($P < 0.0001$) when compared with untreated controls. These data support the conclusion that **12u**-induced cytotoxicity is mediated via the activation of the effector caspase-3.

CLL cells are characterized by resistance to apoptosis mediated by up-regulation of Bcl-2 family proteins. Mcl-1 is the most important antiapoptotic member of the Bcl-2 protein family and is overexpressed in the majority of patients with CLL at baseline. Increased levels of Mcl-1 are associated with both drug resistance and inferior survival.[53,54] Down-regulation of Mcl-1 is sufficient to induce apoptosis in CLL cells.[55] A correlation between lower Mcl-1 protein and mRNA levels with known biologic prognostic markers and improved outcomes in

dx.doi.org/10.1021/jm301475f | J. Med. Chem. 2013, 56, 640−659

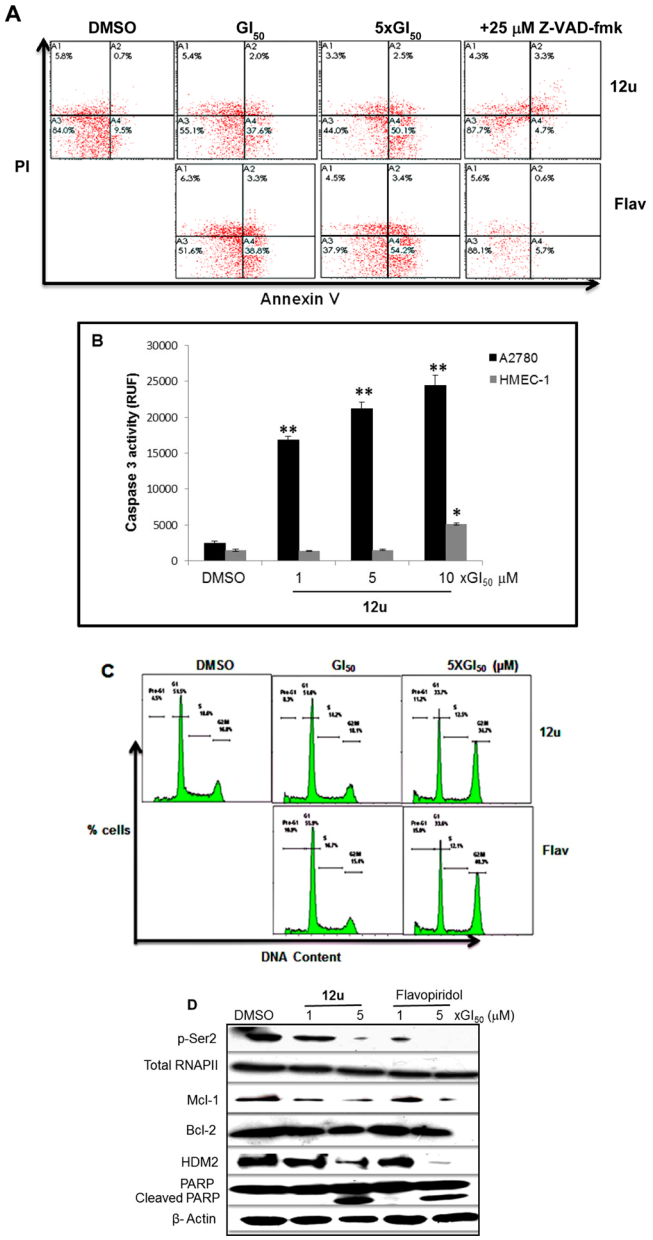

Figure 3. Cellular mode of action of **12u**. (A) A2780 cells were exposed to **12u**, flavopiridol, or **12u** (or flavopiridol) + 25 μM Z-VAD-fmk for 48 h and analyzed by annexin V/PI staining. The percentage of cells undergoing apoptosis was defined as the sum of early apoptosis (annexin V-positive cells) and late apoptosis (annexin V-positive and PI-positive cells). (B) **12u** induces caspase-3 activity in A2780 after treatment for a period of 24 h, but **12u** is less effective in nontransformed endothelial cell line HMEC-1 upon the same treatment. Vertical bars represent the mean ± SD of two independent experiments. Values significantly different from DMSO vehicle control are marked with asterisks: (*) $P < 0.05$; (**) $P < 0.0001$. (C) Cell-cycle analysis of A2780 cells treated with **12u** or flavopiridol for 24 h. (D) Western blot analysis of A2780 cells treated with **12u** or flavopiridol for 24 h. DMSO diluent was used as control in each experiment, and β-actin antibody was used as an internal control.

patients with CLL has been reported.[53,56] In the present study, primary CLL cells derived from 10 patients were cultured with 1 μM **12u** for 8 h and examined for the effect on Mcl-1 protein. Figure 4D shows that the levels of Mcl-1 protein expression are consistently inhibited by **12u** in all CLL patient samples ($P <$ 0.0001) irrespective of stages of the disease. The change in Mcl-1 protein expression precedes evidence of apoptosis induction suggesting that the inhibition is a trigger for apoptosis rather than a consequence of apoptosis induction.

Table 6. Clinical Characteristics of the CLL Patients (n = 10) in This Study

patient characteristics	number
mean age (years)	68
sex (male/female)	7/3
previously untreated/treated	10/0
Binet stage (A/B/C)	8/2/0
IGHV gene mutation (mutated/unmutated)	8/2
CD38 expression (<20%/≥20%)	7/3
ZAP-70 expression (<20%/≥20%)	7/3

CONCLUSION

In this communication we describe the synthesis and SAR of a series of 5-substituted-4-(thiazol-5-yl)-2-(phenylamino)-pyrimidines and 4-(4-substituted-thiazol-5-yl)-*N*-phenylpyrimidin-2-amines. Many compounds inhibit CDK9 activity at low nanomolar concentrations and exhibit very potent antiproliferative activity in tumor cells. Optimization led to the discovery of **12u**, one of the most selective CDK9 inhibitors in the series, being >80-fold more potent for CDK9 versus CDK2. The cocrystal structures of **12u** bound in CDK9/cyclin T and CDK2/cyclin A provide a rationale for the observed potency and selectivity. Compound **12u** was examined in more detail regarding its cellular mode of action. The study demonstrates that by inhibiting cellular RNAPII transcriptional activity, **12u** mediates down-regulation of the antiapoptotic protein Mcl-1, thereby rendering cells sensitive to apoptosis. Significantly, **12u** exhibits excellent antitumor activity in primary CLL cells but shows little toxicity in healthy normal B- and T-cells. In keeping with this finding, Mcl-1 is not detectable in normal B- and T-cells (data not shown), indicating that Mcl-1 may not be a critical regulator of survival in normal lymphocytes. In contrast, CLL cells appear to have a requirement for this protein in order to maintain viability.[53] This study provides a rationale for further development of CDK9 inhibitors for the treatment of CLL and other human malignancies.

EXPERIMENTAL SECTION

Chemistry. Chemical reagents and solvents were obtained from commercial sources. When necessary, solvents were dried and/or purified by standard methods. ^{1}H NMR and ^{13}C NMR spectra were obtained using a Bruker 400 Ultrashield spectrometer at 400 and 100 MHz, respectively. These were analyzed using the Bruker TOPSPIN 2.1 program. Chemical shifts are reported in parts per million relative to internal tetramethylsilane standard. Coupling constants (J) are quoted to the nearest 0.1 Hz. The following abbreviations are used: s, singlet; d, doublet; t, triplet; q, quartet; m, multiplet; br, broad. High resolution mass spectra were obtained using a Waters 2795 single quadrupole mass spectrometer/micromass LCT platform. Purity for final compounds was greater than 95% and was measured using Waters high performance liquid chromatography (Waters 2487 dual λ absorbance detector) with Phenomenex Gemini-NX 5u C18 110A 250 mm × 4.60 mm column, UV detector at 254 nm, using system A (10% MeOH containing 0.1% TFA for 4 min, followed by linear gradient 10−100% MeOH over 6 min at a flow rate of 1 mL/min), system B (10% MeCN containing 0.1% TFA for 2 min, followed by linear gradient 10−100% over 10 min at a flow rate of 1 mL/min), and system C (10% MeCN containing 0.1% TFA for 4 min, followed by linear gradient 10−100% over 10 min at a flow rate of 1 mL/min).

dx.doi.org/10.1021/jm301475f | J. Med. Chem. 2013, 56, 640−659

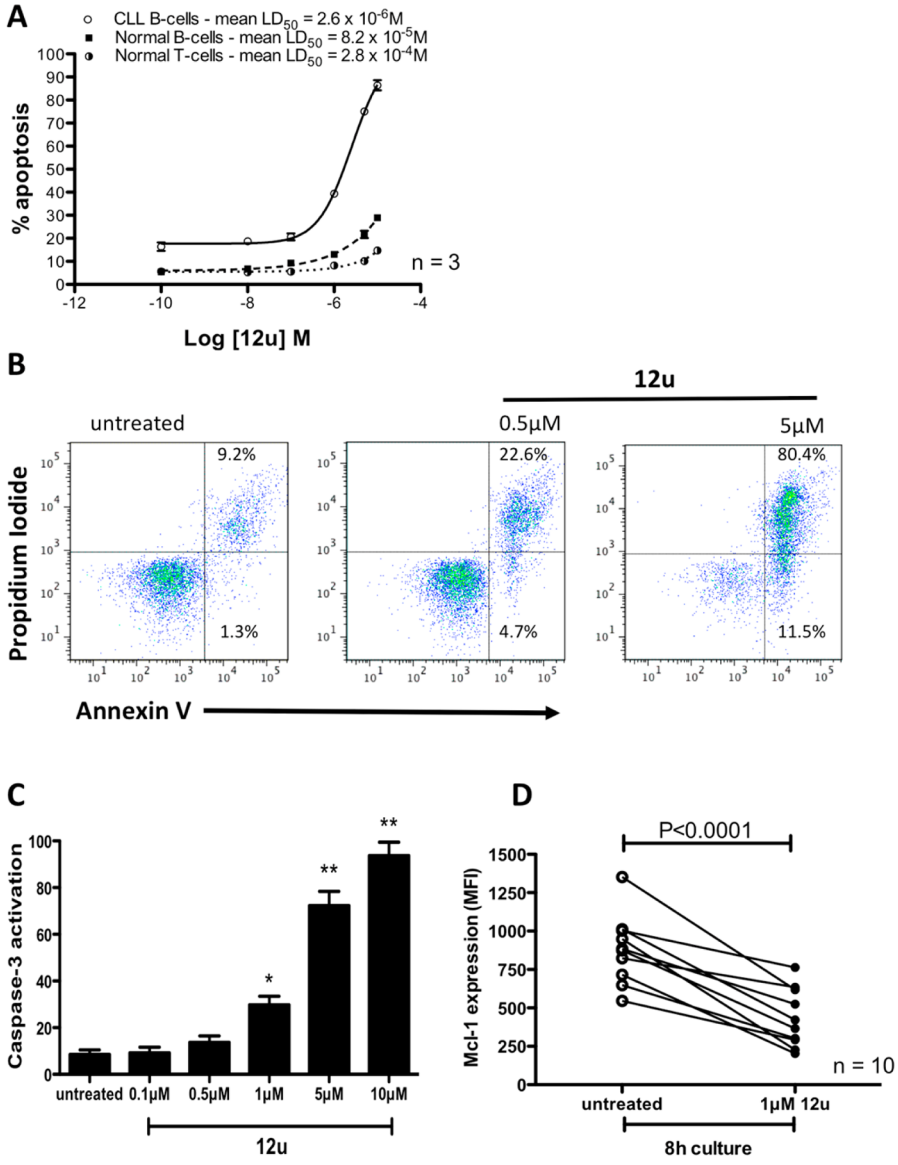

Figure 4. Compound **12u** shows selective toxicity against CLL cells and induces its effects through the induction of apoptosis. Primary CLL cells and normal B-cells were cultured in the presence of increasing concentrations of **12u** for 48 h. (A) Sigmoidal dose−response curves for **12u** in CLL cells and normal B-cells and T-cells. (B) Compound **12u** caused a dose-dependent increase in annexin V-positive cells, and this was preceded by (C) a dose-dependent increase in caspase-3 activation after 24 h in culture ((∗) $P < 0.05$, (∗∗) $P < 0.0001$). (D) Mcl-1 protein expression was significantly inhibited by **12u** at 8 h in all the primary CLL samples tested ($P < 0.0001$).

Flash chromatography was performed using either a glass column packed with silica gel (200−400 mesh, Aldrich Chemical) or prepacked silica gel cartridges (FlashMaster systems, Biotage). Melting points were determined with an Electrothermal melting point apparatus.

Ethyl 4-Methyl-2-(methylamino)thiazole-5-carboxylate 1. To a solution of ethyl 2-chloroacetoacetate (13.8 mL, 100 mmol) in 100 mL of MeOH were added 1-methylthiourea and 3 mL of pyridine, and the mixture was stirred at room temperature for 4 h. The mixture was concentrated and the precipitate was washed with saturated $NaHCO_3$ solution, filtered, and dried to offer the title compound as a white solid (17.46 g, 85% yield), mp 88−90 °C. ^{1}H NMR ($CDCl_3$): δ 1.35 (t, 3H, J = 7.2 Hz, CH_3), 2.53 (s, 3H, CH_3), 2.99 (s, 3H, CH_3), 4.28 (q, 2H, J = 7.2 Hz, CH_2). ^{13}C NMR ($CDCl_3$): δ 14.78, 17.67, 31.27, 60.28, 107.47, 159.79, 162.37, 171.08. HR-MS (ESI^+): m/z $[M + H]^+$ calcd for $C_8H_{13}N_2O_2S$, 201.0698, found 201.0463.

Ethyl 2-(*tert*-Butoxycarbonyl(methyl)amino)-4-methylthiazole-5-carboxylate 2. To a solution of ethyl 4-methyl-2-(methylamino)thiazole-5-carboxylate (10.0 g, 50.0 mmol) in DCM were added 4-dimethylaminopyridine (DMAP) (1.0 g) and di-*tert*-butyl dicarbonate (12.0 g, 55.0 mmol), and the reaction was continued for 8 h at room temperature. After completion of the reaction, the mixture was washed with 5% aqueous HCl, followed by saturated $NaHCO_3$ solution, brine, dried over $MgSO_4$, and filtered. The organic solution was concentrated to dryness, and the title compound was obtained via recrystallization from hexane as a white solid (14 g, 93%), mp 148−150 °C. ^{1}H NMR ($CDCl_3$): δ 1.34 (t, 3H, J = 7.2 Hz, CH_3), 1.60 (s, 9H, 3 × CH_3), 2.64 (s, 3H, CH_3), 3.55 (s, 3H, CH_3), 4.29 (q, 2H, J = 7.2 Hz, CH_2). ^{13}C NMR ($CDCl_3$): δ 14.35, 17.37, 28.14, 33.94, 60.54, 83.85, 116.19, 153.13, 156.56, 162.68, 163.10. HR-MS (ESI^+): m/z $[M + H]^+$ $C_{13}H_{21}N_2O_4S$, 301.1222, found 301.1312.

***tert*-Butyl 5-(2-Cyanoacetyl)-4-methylthiazol-2-yl(methyl)-carbamate 3.** To a solution of **2** (6.0 g, 20.0 mmol) in 6 mL of anhydrous THF was added 1.50 mL of acetonitrile (1.3 mmol). The mixture was cooled at −78 °C, and LDA was added dropwise over 10 min. The reaction was continued for 2 h. After completion of the reaction, 10 mL of H_2O was added and the mixture was acidified with dilute HCl solution and extracted with $CHCl_3$ (3 × 50 mL). The

dx.doi.org/10.1021/jm301475f | J. Med. Chem. 2013, 56, 640−659

combined organic phase was washed with brine, dried over $MgSO_4$, and concentrated to dryness. The mixture was purified by using PE/EtOAc as elutant to afford the title compound as a white solid (4.25 g, 72%), mp 119−121 °C. ^{1}H NMR ($CDCl_3$): δ 1.61 (s, 9H, 3 × CH_3), 2.68 (s, 3H, CH_3), 3.59 (s, 3H, CH_3), 3.86 (s, 2H, CH_2). ^{13}C NMR ($CDCl_3$): δ 18.71, 28.09, 32.23, 34.26, 84.76, 113.76, 122.37, 153.11, 159.36, 163.14, 179.25. HR-MS (ESI^+): m/z $[M + H]^+$ calcd for $C_{13}H_{18}N_3O_3S$, 296.1069, found 296.1130.

***tert*-Butyl (5-(2-Cyano-3-(dimethylamino)acryloyl)-4-methylthiazol-2-yl)(methyl)carbamate (4, R^1 = Boc, R′ = CN).** The compound was prepared by the method described previously.[35] Yellow solid (80% yield), mp 174−176 °C. ^{1}H NMR ($CDCl_3$): δ 1.59 (s, 9H, 3 × CH_3), 2.56 (s, 3H, CH_3), 3.28 (s, 3H, CH_3), 3.46 (s, 3H, CH_3), 3.54 (s, 3H, CH_3), 7.86 (s, 1H, CH). ^{13}C NMR ($CDCl_3$): δ 18.33, 28.18, 34.09, 38.97, 48.17, 81.56, 83.89, 119.49, 124.63, 152.80, 153.07, 158.71, 161.97, 182.43. HR-MS (ESI^+): m/z $[M + H]^+$ calcd for $C_{16}H_{23}N_4O_3S$, 351.1491, found 351.1281.

3-(Dimethylamino)-2-fluoro-1-(4-methyl-2-(methylamino)-thiazol-5-yl)prop-2-en-1-one (4, R′ = F). To a well-stirred solution of 3-(dimethylamino)-1-(4-methyl-2-(methylamino)thiazol-5-yl)prop-2-en-1-one (**6**)[35] (5.0 mmol) in MeOH under ice bath was added SelecFluor (7.5 mmol), and the mixture was stirred for 1 h. After completion of the reaction, the mixture was concentrated and purified by column chromatography using EtoAc/MeOH to yield the title compound. Yellow solid (30%). ^{1}H NMR (DMSO-d_6): δ 2.40 (s, 3H, CH_3), 2.83 (d, 3H, J = 4.8 Hz, CH_3), 3.04 (apparent s, 6H, 2 × CH_3), 6.88 (d, 1H, J = 30.4 Hz, CH), 8.04 (d, 1H, J = 4.4 Hz, NH). HR-MS (ESI^+): m/z $[M + H]^+$ calcd for $C_{10}H_{15}FN_3OS$, 244.0920, found 244.0849.

(2-Chloro-3-(dimethylamino)-1-(4-methyl-2-(methylamino)-thiazol-5-yl)prop-2-en-1-one (4, R′ = Cl). To an ice-cooled solution of **6** (2.0 mmol) in 50 mL of methanol was added *N*-chlorosuccinmide (20 mmol) over 10 min dropwise. After being stirred at room temperature for 30 min, the mixture was concentrated and purified by column chromatography using EtoAc to yield the title compound as a light yellow solid (43%), mp 141−143 °C. ^{1}H NMR ($CDCl_3$): δ 2.38 (s, 3H, CH_3), 2.99 (s, 3H, CH_3), 3.26 (s, 6H, 2 × CH_3), 6.44 (s, 1H, NH), 7.42 (s, 1H, CH). ^{13}C NMR ($CDCl_3$): δ 18.28, 31.98, 43.33, 101.88, 117.86, 149.13, 153.84, 171.91, 180.77. HR-MS (ESI^+): m/z $[M + H]^+$ calcd for $C_{10}H_{15}ClN_3OS$, 260.0624, found 260.0541.

***tert*-Butyl Methyl(4-methylthiazol-2-yl)carbamate (8).** *N*,4-Dimethylthiazol-2-amine was obtained from 1-methylthiourea and 1-chloropropan-2-one using the method for preparing **1** as off-white solid (88%), mp 68−70 °C. ^{1}H NMR ($CDCl_3$): δ 2.96 (d, 3H, J = 1.2 Hz, CH_3), 2.96 (s, 3H, CH_3), 6.06 (q, 1H, J = 1.2 Hz, CH), 6.15 (brs, 1H, NH). ^{13}C NMR ($CDCl_3$): δ 17.36, 31.95, 100.06, 148.66, 171.61. HR-MS (ESI^+): m/z $[M + H]^+$ calcd for $C_5H_9N_2OS$, 129.0486, found 129.0372. The title compound was obtained from *N*,4-dimethylthiazol-2-amine and di-*tert*-butyl dicarbonate by the method for preparing **2** as light yellow liquid (55%). ^{1}H NMR ($CDCl_3$): δ 1.59 (s, 9H, 2 × CH_3), 2.35 (d, 3H, J = 1.2 Hz, CH_3), 3.55 (s, 3H, CH_3), 6.48 (q, 1H, J = 0.8 Hz, CH). ^{13}C NMR ($CDCl_3$): δ 17.41, 28.20, 34.32, 82.91, 108.39, 147.11, 153.13, 161.20. HR-MS (ESI^+): m/z $[M -$ *tert*-butyl $+ H]^+$ calcd for $C_6H_9N_2O_2S$, 173.0385, found 173.0224.

General Procedure for Preparation of 9 (R′ = Me, Et, or Pr). To a solution of **8** (10.0 mmol) in 15 mL of anhydrous THF cooling at −78 °C was added 25.0 mmol of LDA dropwise. After the mixture was stirred for 30 min the corresponding aldehyde (12.0 mmol) was added and the reaction was continued for a further 1 h. After completion of the reaction, 10 mL of water was added and the mixture was washed with 2 M aqueous HCl solution. After removal of THF, the mixture was extracted with $CHCl_3$ (3 × 30 mL) and the combined organic layers were washed with brine, dried over $MgSO_4$, filtered, and concentrated to dryness. The title compound was obtained by column chromatography using EtOAc/PE as eluant.

***tert*-Butyl 5-(1-Hydroxypropyl)-4-methylthiazol-2-yl-(methyl)carbamate (9, R′ = Me).** Light yellow liquid (63%). ^{1}H NMR ($CDCl_3$): δ 0.94 (t, 3H, J = 7.2 Hz, CH_3), 1.28−1.48 (m, 2H, CH_2), 1.58 (s, 9H, 3 × CH_3), 1.67−1.94 (m, 3H, CH_2 and OH), 2.30 (s, 3H, CH_3), 3.51 (s, 3H, CH_3), 4.81 (t, 1H, J = 7.2 Hz, CH). HR-MS (m/z): calcd for $C_{13}H_{22}N_2O_3S$, 287.1429; found 287.1503 $[M + H]^+$.

***tert*-Butyl (5-(1-Hydroxybutyl)-4-methylthiazol-2-yl)-(methyl)carbamate (9, R′ = Et).** Light yellow liquid (77%). ^{1}H NMR ($CDCl_3$): δ 0.94 (t, 3H, J = 7.2 Hz, CH_3), 1.24−1.48 (m, 2H, CH_2), 1.59 (s, 9H, 3 × CH_3), 1.67−1.94 (m, 3H, OH and CH_2), 1.94 (s, 1H, OH), 2.30 (s, 3H, CH_3), 3.51 (s, 3H, CH_3), 4.89 (t, 1H, J = 7.2 Hz, CH). HR-MS (ESI^+): m/z $[M + H]^+$ calcd for $C_{14}H_{25}N_2O_3S$, 301.1586, found 301.1650.

***tert*-Butyl (5-(1-Hydroxypentyl)-4-methylthiazol-2-yl)-(methyl)carbamate (9, R′ = Pr).** Light yellow liquid (53%). ^{1}H NMR ($CDCl_3$): δ 0.91 (t, 3H, J = 7.2 Hz, CH_3), 1.23−1.43 (m, 4H, 2 × CH_2), 1.59 (s, 9H, 3 × CH_3), 1.71−1.98 (m, 3H, CH_2 and OH), 2.31 (s, 3H, CH_3), 3.52 (s, 3H, CH_3), 4.89 (t, 1H, J = 7.2 Hz, CH). HR-MS (ESI^+): m/z $[M + H]^+$ calcd for $C_{15}H_{27}N_2O_3S$, 315.1742, found 315.1776.

General Procedure for Preparation of 10 (R′ = Me, Et, or Pr). A solution of corresponding **9** in $CHCl_3$ (1.5 mmol/mL) was treated with MnO_2 (5.0 equiv), and the mixture was refluxed for 3 h. Upon completion of the reaction, the mixture was filtered through Celite, and the filtrate was concentrated to dryness.

***tert*-Butyl Methyl(4-methyl-5-propionylthiazol-2-yl)-carbamate (10, R′ = Me).** Yellow solid (85%), mp 97−99 °C. ^{1}H NMR ($CDCl_3$): δ 1.20 (t, 3H, J = 7.2 Hz, CH_3), 1.61 (s, 9H, 3 × CH_3), 2.66 (s, 3H, CH_3), 2.78 (q, 2H, J = 7.2 Hz, CH_2), 3.57 (s, 3H, CH_3). ^{13}C NMR ($CDCl_3$): δ 8.36, 18.40, 28.15, 34.08, 36.01, 84.03, 125.02, 153.14, 155.40, 161.74, 194.13. HRMS (ESI^+): m/z $[M + H]^+$ $C_{13}H_{21}N_2O_3S$, 285.1273, found 285.1183.

***tert*-Butyl (5-Butyryl-4-methylthiazol-2-yl)(methyl)-carbamate (10, R′ = Et).** Yellow solid (81%), mp 101−103 °C. ^{1}H NMR ($CDCl_3$): δ 0.99 (t, 3H, J = 7.2 Hz, CH_3), 1.61 (s, 9H, 3 × CH_3), 1.70−1.82 (m, 2H, CH_2), 2.67 (s, 3H, CH_3), 2.76 (t, 2H, J = 7.2 Hz, CH_2), 3.57 (s, 3H, CH_3). ^{13}C NMR ($CDCl_3$): δ 13.79, 17.92, 18.35, 28.15, 34.12, 44.93, 84.06, 125.21, 153.14, 155.37, 161.72, 193.63. HR-MS (ESI^+): m/z $[M + H]^+$ $C_{14}H_{23}N_2O_3S$, 299.1429, found 299.1459.

***tert*-Butyl Methyl(4-methyl-5-pentanoylthiazol-2-yl)-carbamate (10, R′ = Pr).** Yellow solid (65%), mp 82−84 °C. ^{1}H NMR ($CDCl_3$): δ 0.92 (t, 3H, J = 7.2 Hz, CH_3), 1.30−1.43 (m, 2H, CH_2), 1.59 (s, 9H, 3 × CH_3), 1.62−1.72 (m, 2H, CH_2), 2.64 (s, 3H, CH_3), 2.75 (t, 2H, J = 7.2 Hz, CH_2), 3.55 (s, 3H, CH_3). ^{13}C NMR ($CDCl_3$): δ 13.88, 18.38, 22.37, 26.54, 28.14, 34.07, 42.73, 84.01, 125.16, 153.16, 155.50, 161.67, 193.78. HR-MS (ESI^+): m/z $[M + H]^+$ $C_{15}H_{25}N_2O_3S$, 313.1586, found 313.1620.

Preparations of **4** (R^1 = Boc, R′ = Me, Et or Pr) were done by heating **10** in DMF−DMA using the method described previously[35] or by heating in a Discovery microwave at 140 °C for 45 min. The mixture was concentrated and used for the pyrimidine formation reaction without further purification.

General Procedure for Preparation of Ic and 12a−u. A mixture of the appropriate 3-(dimethylamino)-1-(4-methyl-2-(methylamino)thiazol-5-yl)prop-2-en-1-one or **4** and 1-phenylguanidine (**11**)[32,35] (2 equiv mmol) in 2-methoxyethanol (0.2 mL/mmol) was heated in a microwave at 100−140 °C for 20−45 min. When the mixture was cooled, the residue was purified by flash chromatography using appropriate mixtures of EtoAc/PE or EtoAc/MeOH as the eluant. The products were further purified by crystallization from EtOAc−MeOH mixtures.

4-(4-Methyl-2-(methylamino)thiazol-5-yl)-2-(3-nitrophenylamino)pyrimidine-5-carbonitrile (12a). **12a** was obtained from *tert*-butyl (5-(2-cyano-3-(dimethylamino)acryloyl)-4-methylthiazol-2-yl)(methyl)carbamate and 1-(3-nitrophenyl)guanidine hydrochloride. Yellow solid (39%); mp 304−305 °C. Anal. RP-HPLC: t_R 12.94 min (method A), 12.34 min (method C), purity 99%. ^{1}H NMR (DMSO-d_6): δ 2.45 (s, 3H, CH_3), 2.91 (d, 3H, J = 4.4 Hz, CH_3), 7.63 (t, 1H, J = 8.0 Hz, Ph-H), 7.91 (dt, 1H, J = 8.0, 1.6 Hz, Ph-H), 8.06 (d, 1H, J = 7.6 Hz, Ph-H), 8.34 (q, 1H, J = 4.4 Hz, NH), 8.84 (s, 1H, Ph-H), 8.88 (s, 1H, Py-H), 10.68 (s, 1H, NH). ^{13}C NMR (DMSO-d_6): δ 20.03, 31.39, 95.05, 114.44, 117.74, 117.99, 126.51, 130.35, 140.84, 148.49, 156.48, 159.11, 161.43, 164.19, 170.99. HR-

dx.doi.org/10.1021/jm301475f | J. Med. Chem. 2013, 56, 640−659

MS (ESI$^+$): m/z [M + H]$^+$ calcd for $C_{16}H_{14}N_7O_2S$, 368.0930, found, 368.0840.

4-(4-Methyl-2-(methylamino)thiazol-5-yl)-2-((3-nitrophenyl)amino)pyrimidin-5-ol (12b). **12b** was obtained from 2-chloro-3-(dimethylamino)-1-(4-methyl-2-(methylamino)thiazol-5-yl)prop-2-en-1-one and 1-(3-nitrophenyl) guanidine. Yellow solid (6%); mp 210−211 °C. Anal. RP-HPLC: t_R 10.95 min (method A), 10.78 min (method C), purity 97%. ^{1}H NMR (DMSO-d_6): δ 2.32 (s, 3H, CH_3), 2.86 (d, 3H, J = 4.8 Hz, CH_3), 6.42 (s, 2H, NH and OH), 7.53 (s, 1H, Py-H), 7.71 (dt, 2H,, J = 8.0, 1.6 Hz, Ph-H), 7.75 (t, 1H, J = 8.0 Hz, Ph-H), 8.12 (t, 1H, J = 2.0 Hz, Ph-H), 8.19 (q, 1H, J = 4.8 Hz, NH), 8.30−8.26 (m, 1H, Ph-H). ^{13}C NMR (DMSO-d_6): δ 18.89, 31.31, 116.43, 122.88, 123.22, 128.78, 130.97, 134.79, 137.80, 139.01, 148.64, 154.79, 157.72, 170.63, 172.04. HR-MS (ESI$^+$): m/z [M + H]$^+$ calcd for $C_{15}H_{15}N_6O_3S$, 359.0926, found, 359.0688.

3-(5-Cyano-4-(4-methyl-2-(methylamino)thiazol-5-yl)-pyrimidin-2-ylamino)benzenesulfonamide (12c). **12c** was obtained from *tert*-butyl (5-(2-cyano-3-(dimethylamino)acryloyl)-4-methylthiazol-2-yl)(methyl)carbamate and 3-guanidinobenzenesulfonamide. Gray solid (76%); mp 314−315 °C. Anal. RP-HPLC: t_R 11.25 min (method A), 11.25 (method C), purity 99%. ^{1}H NMR (DMSO-d_6): δ 2.45 (s, 3H, CH_3), 2.90 (d, 3H, J = 4.8 Hz, CH_3), 7.36 (s, 2H, NH_2), 7.50−7.57 (m, 2H, 2 × Ph-H), 7.88−7.95 (m, 1H, Ph-H), 8.25 (s, 1H, Ph-H), 8.29 (q, 1H, J = 4.8 Hz, NH), 8.82 (s, 1H, Py-H), 10.49 (s, 1H, NH). ^{13}C NMR (DMSO-d_6): δ 20.07, 31.37, 94.51, 117.71, 118.16, 120.62, 123.80, 129.73, 139.85, 145.06, 156.63, 159.30, 161.44, 164.17, 170.89. HR-MS (ESI$^+$): m/z [M + H]$^+$ calcd for $C_{16}H_{16}N_7O_2S_2$, 402.0870, found, 402.0970.

3-((5-Hydroxy-4-(4-methyl-2-(methylamino)thiazol-5-yl)-pyrimidin-2-yl)amino)benzen esulfonamide (12d). **12d** was obtained from 2-chloro-3-(dimethylamino)-1-(4-methyl-2-(methylamino)thiazol-5-yl)prop-2-en-1-one and 3-guanidinobenzenesulfonamide. Gray solid (6%); mp 254−256 °C. Anal. RP-HPLC: t_R 10.12 min (method A), 10.10 (method C), purity 100%. ^{1}H NMR (DMSO-d_6): δ 2.32 (s, 3H, CH_3), 2.86 (d, 3H, J = 4.8 Hz, CH_3), 6.26 (s, 2H, NH & OH), 7.41−7.52 (m, 4H, Ph-H and Py-H and NH_2), 7.63 (t, 1H, J = 1.6 Hz, Ph-H), 7.67 (t, 1H, J = 8.0 Hz, Ph-H), 7.84 (dt, 1H, J = 8.0, 1.6 Hz, Ph-H), 8.19 (q, 1H, J = 4.8 Hz, NH). ^{13}C NMR (DMSO-d_6): δ 18.88, 31.31, 116.64, 124.25, 125.43, 128.92, 130.51, 131.17, 137.11, 138.85, 145.31, 154.70, 157.60, 170.61, 172.07. HR-MS (ESI$^+$): m/z [M + H]$^+$ calcd for $C_{15}H_{17}N_6O_3S_2$, 393.0804, found, 393.0883.

3-(5-Fluoro-4-(4-methyl-2-(methylamino)thiazol-5-yl)-pyrimidin-2-ylamino)benzenesulfonamide (12e). **12e** was obtained from 3-guanidinobenzenesulfonamide and 3-(dimethylamino)-2-fluoro-1-(4-methyl-2-(methylamino)thiazol-5-yl)prop-2-en-1-one. Yellow solid (24%); mp 268−270 °C. Anal. RP-HPLC: t_R 11.45 min (method A), 9.12 min (method B), purity 99%. ^{1}H NMR (DMSO-d_6): δ 2.48 (s, 3H, CH_3), 2.88 (d, 3H, J = 4.8 Hz, CH_3), 7.29 (s, 2H, NH_2), 7.40 (d, 1H, J = 8.0 Hz, Ph-H), 7.47 (t, 1H, J = 8.0 Hz, Ph-H), 7.89 (d, 1H, J = 8.0 Hz, Ph-H), 8.13 (brs q, 1H, J = 4.8 Hz, NH), 8.25 (s, 1H, Ph-H), 8.47 (d, 1H, J = 3.2 Hz, Py-H), 9.83 (s, 1H, NH). ^{13}C NMR (DMSO-d_6): δ 19.43 (d, J = 5 Hz), 31.33, 109.97 (d, J = 8 Hz), 115.81, 118.78, 121.89, 129.51, 141.46, 144.94, 145.97 (d, J = 25 Hz), 147.63 (d, J = 12 Hz), 147.94 (d, J = 248 Hz), 155.66, 156.04, 171.34. HR-MS (ESI$^+$): m/z [M + H]$^+$ calcd for $C_{15}H_{16}FN_6O_2S_2$, 395.0760, found 395.0641.

3-((5-Chloro-4-(4-methyl-2-(methylamino)thiazol-5-yl)-pyrimidin-2-yl)amino)benzenesulfonamide (12f). **12f** was obtained from 3-guanidinobenzenesulfonamide and 2-chloro-4-methyl-1-(4-methyl-2-(methylamino)thiazol-5-yl)pent-2-en-1-one. Yellow solid (10%); mp 165 °C (dec). Anal. RP-HPLC: t_R 11.45 min (method A), 11.40 min (method C), purity 98%. ^{1}H NMR (MeOH-d_4): δ 2.44 (s, 3H, CH_3), 2.99 (s, 3H, CH_3), 7.46 (t, 1H, J = 8.0 Hz, Ph-H), 7.52−7.57 (m, 1H, Ph-H), 7.81−7.87 (m, 1H, Ph-H), 8.41 (t, 1H, J = 1.2 Hz, Ph-H), 8.42 (s, 1H, Py-H). HRMS (ESI$^+$): m/z [M + H]$^+$ calcd for $C_{15}H_{16}ClN_6O_2S_2$, 411.0465; found 411.0530.

3-((5-Methyl-4-(4-methyl-2-(methylamino)thiazol-5-yl)-pyrimidin-2-yl)amino)benzenesulfonamide (12g). **12g** was obtained from 3-guanidinobenzenesulfonamide and 3-(dimethylamino)-2-methyl-1-(4-methyl-2-(methylamino)thiazol-5-yl)prop-2-en-1-one. Light orange solid (76%); mp 224−226 °C. Anal. RP-HPLC: t_R 11.02 min (method A), 8.87 (method B), purity 99%. ^{1}H NMR (DMSO-d_6): δ 2.20 (s, 3H, CH_3), 2.24 (s, 3H, CH_3), 2.86 (d, 1H, J = 4.8 Hz, CH_3), 7.28 (s, 1H, NH_2), 7.37 (dt, 1H, J = 8.0, 1.2 Hz, Ph-H), 7.45 (t, 1H, J = 8.0 Hz, Ph-H), 7.78 (q, 1H, J = 4.8 Hz, NH), 7.93−8.00 (m, 1H, Ph-H), 8.30 (s, 1H, J = 2.0 Hz, Ph-H), 8.37 (s, 1H, Py-H), 9.76 (s, 1H, NH). ^{13}C NMR (DMSO-d_6): δ 16.71, 18.19, 31.29, 114.68, 115.60, 118.36, 119.07, 121.56, 129.48, 141.75, 144.94, 150.52, 158.26, 158.94, 160.21, 169.57. HRMS (ESI$^+$): m/z [M + H]$^+$ calcd for $C_{16}H_{19}N_6O_2S_2$, 391.1011, found 391.1020.

3-((5-Ethyl-4-(4-methyl-2-(methylamino)thiazol-5-yl)-pyrimidin-2 yl)amino)benzenesulfonamide (12h). **12h** was obtained from *tert*-butyl (5-(2-((dimethylamino)methylene)-butanoyl)-4-methylthiazol-2-yl)(methyl)carbamate and 3-guanidinobenzenesulfonamide. Light yellow powder (30%); mp 183−185 °C. Anal. RP-HPLC: t_R 11.32 min (method A), 9.12 min (method B), purity 100%. ^{1}H NMR (DMSO-d_6): δ 1.10 (t, 1H, J = 7.6 Hz, CH_3), 2.20 (s, 3H, CH_3), 2.59 (q, 2H, J = 7.6 Hz, CH_2), 2.85 (d, 1H, J = 4.8 Hz, CH_3), 7.28 (s, 1H, NH_2), 7.38 (dt, 1H, J = 8.0, 1.6 Hz, Ph-H), 7.45 (t, 1H, J = 8.0 Hz, Ph-H), 7.74 (q, 1H,, J = 4.8 Hz, NH), 7.93−8.00 (m, 1H, Ph-H), 8.31 (t, 1H, J = 1.6 Hz, Ph-H), 8.43 (s, 1H, Py-H), 9.82(s, 1H, NH). ^{13}C NMR (DMSO-d_6): δ 15.46, 17.72, 22.93, 31.28, 113.99, 115.61, 118.40, 121.54, 125.64, 129.49, 141.70, 144.95, 149.80, 158.26, 158.46, 159.40, 169.20. HR-MS (ESI$^+$): m/z [M + H]$^+$ calcd for $C_{17}H_{21}N_6O_2S_2$, 405.1167, found 405.0863.

3-((4-(4-Methyl-2-(methylamino)thiazol-5-yl)-5-propylpyrimidin-2-yl)amino)benzenesulfonamide (12i). **12i** was obtained from *tert*-butyl (5-(2-((dimethylamino)methylene)pentanoyl)-4-methylthiazol-2-yl)(methyl)carbamate and 3-guanidinobenzenesulfonamide. Yellow solid (30%); mp 160−162 °C. Anal. RP-HPLC: t_R 11.52 min (method A), 11.57 min (method C), purity 100%. ^{1}H NMR (DMSO-d_6): δ 0.85 (t, 1H, J = 7.6 Hz, CH_3), 1.42−1.54 (m, 2H, CH_2), 2.21 (s, 3H, CH_3), 2.55 (t, 2H, J = 7.6 Hz, CH_2), 2.85 (d, 1H, J = 4.8 Hz, CH_3), 7.28 (s, 1H, NH_2), 7.37 (dt, 1H, J = 8.0, 1.6 Hz, Ph-H), 7.45(t, 1H, J = 8.0 Hz, Ph-H), 7.92−8.00 (m, 1H, Ph-H), 8.30 (t, 1H, J = 1.6 Hz, Ph-H), 8.40 (s, 1H, Py-H), 9.81(s, lH, NH). ^{13}C NMR (DMSO-d_6): δ 14.11, 17.71, 23.80, 31.26, 31.64, 114.08, 115.59, 118.40, 121.55, 124.04, 129.49, 141.68, 144.94, 149.80, 158.29, 158.69, 159.76, 169.15. HR-MS (ESI$^+$): m/z [M + H]$^+$ calcd for $C_{18}H_{23}N_6O_2S_2$, 419.1324, found 419.0733.

2-(3-(4-Acetylpiperazin-1-yl)phenylamino)-4-(4-methyl-2-(methylamino)thiazol-5-yl)pyrimidine-5-carbonitrile (12j). **12j** was obtained from 1-(3-acetylpiperazin-1-yl)phenyl)guanidine and *tert*-butyl (5-(2-cyano-3-(dimethylamino)acryloyl)-4-methylthiazol-2-yl)(methyl)carbamate. Yellow solid (58%); mp 241−243 °C. Anal. RP-HPLC: t_R 12.10 min (method A), 9.02 min (method B), purity 100%. ^{1}H NMR (DMSO-d_6): δ 2.05 (s, 3H, CH_3), 2.40 (brs, 3H, CH_3), 2.89 (d, 3H, J = 4.4 Hz, CH_3), 3.10 (apparent t, 2H, J = 5.2 Hz, CH_2), 3.17 (apparent t, 2H, J = 5.2 Hz, CH_2), 3.54−3.62 (m, 4H, 2 × CH_2), 6.62−6.73 (m, 1H, Ph-H), 7.12−7.24 (m, 2H, 2 × Ph-H), 7.40 (br s, 1H, Ph-H), 8.25 (brq, 1H, J = 4.8 Hz, NH), 8.77 (s, 1H, Py-H), 10.12 (brs, 1H, NH). ^{13}C NMR (DMSO-d_6): δ 19.93, 21.65, 31.35, 41.12, 45.90, 48.87, 49.31, 94.05, 108.65, 111.62, 112.38, 118.28, 129.47, 140.09, 151.66, 159.46, 161.56, 163.89, 168.80, 170.68. HR-MS (ESI$^+$): m/z [M + H]$^+$ calcd for $C_{22}H_{25}N_8OS$, 449.1872, found 449.1727.

4-(4-Methyl-2-(methylamino)thiazol-5-yl)-2-(3-(piperazin-1-yl)phenylamino)pyrimidine-5-carbonitrile (12k). A mixture of **12j** in methanol (5 mL) and 2 M HCl (4 mL) was heated under reflux for 3 h. After completion of the reaction, the mixture was neutralized by NaOH solution, extracted with chloroform, and purified by column chromatography using chloroform/MeOH as the eluant to get the final product. Yellow solid (57%); mp 160−162 °C. Anal. RP-HPLC: t_R 11.09 min (method A), 8.65 min (method B), purity 98%. ^{1}H NMR (DMSO-d_6): δ 2.39 (s, 3H, CH_3), 2.83 (apparent t, 4H, J = 4.4 Hz, 2 × CH_2), 2.89 (s, 3H, CH_3), 3.04 (apparent t, 2H, J = 4.4 Hz, 2 × CH_2), 6.55−7.70 (t, 1H, J = 2.0 Hz, Ph-H), 7.02−7.22 (m, 2H, 2 × Ph-H), 7.36 (br s, 1H, Ph-H), 8.25 (br s, 1H, NH), 8.77 (s, 1H, Py-H), 10.08 (br s, 1H, NH). ^{13}C NMR (DMSO-d_6): δ 19.92, 31.35, 46.08,

dx.doi.org/10.1021/jm301475f | J. Med. Chem. 2013, 56, 640−659

50.01, 93.99, 108.06, 111.10, 111.71, 118.30, 129.32, 140.01, 152.56, 159.46, 161.58, 163.85, 170.66. HR-MS (ESI$^+$): m/z [M + H]$^+$ calcd for $C_{20}H_{23}N_8S$, 407.1766, found 407.1874.

2-(4-(4-Acetylpiperazin-1-yl)phenylamino)-4-(4-methyl-2-(methylamino)thiazol-5-yl)pyrimidine-5-carbonitrile (12l). 12l was obtained from 1-(4-acetylpiperazin-1-yl)phenyl)guanidine and *tert*-butyl (5-(2-cyano-3-(dimethylamino)acryloyl)-4-methylthiazol-2-yl)(methyl)carbamate. Yellow solid (23%); mp 226−228 °C. Anal. RP-HPLC: t_R 11.69 min (method A), 8.67 min (method B), purity 98%. ^{1}H NMR (DMSO-d_6): δ 2.05 (s, 3H, CH_3), 2.38 (br s, 3H, CH_3), 2.89 (d, 3H, J = 4.8 Hz), 3.05 (apparent t, 2H, J = 4.8 Hz, CH_2), 3.12 (apparent t, 2H, J = 4.8 Hz, CH_2), 3.51−3.63 (m, 4H, 2 × CH_2), 6.95 (d, 2H, J = 9.2 Hz, 2 × Ph-H), 7.55 (d, 2H, J = 8.8 Hz, 2 × Ph-H), 8.21 (br q, 1H, J = 4.8 Hz, NH), 8.71 (s, 1H, Py-H), 10.08 (br s, 1H, NH). ^{13}C NMR (DMSO-d_6): δ 19.91, 21.65, 31.29, 41.14, 45.95, 49.21, 49.63, 93.28, 116.57, 118.48, 122.40, 124.24, 131.47, 147.63, 155.52, 159.44, 161.47, 163.91, 168.74, 170.49. HR-MS (ESI$^+$): m/z [M + H]$^+$ calcd for $C_{22}H_{25}N_8OS$, 449.1872, found 449.1940.

4-(4-Methyl-2-(methylamino)thiazol-5-yl)-2-(4-(piperazin-1-yl)phenylamino)pyrimidine-5-carbonitrile (12m). 12m was obtained from 2-(4-(4-acetylpiperazin-1-yl)phenylamino)-4-(4-methyl-2-(methylamino)thiazol-5-yl)pyrimidine-5-carbonitrile. Yellow solid (80%); mp 192−194 °C. Anal. RP-HPLC: t_R 10.92 min (method A), 8.35 min (method B), purity 96%. ^{1}H NMR (DMSO-d_6) δ: 2.39 (s.3H, CH_3), 2.88 (d, 3H, J = 4.8 Hz), 3.08−3.17 (m, 4H, 2 × CH_2), 3.20−3.28 (m, 4H, 2 × CH_2), 6.96 (d, 2H, J = 8.8 Hz, 2 × Ph-H), 7.56 (d, 2H, J = 8.8 Hz, 2 × Ph-H), 8.24 (q, 1H, J = 4.8 Hz, NH), 8.71 (s, 1H, Py-H), 10.09 (bs, 1H, NH). ^{13}C NMR (DMSO-d_6): δ 19.92, 31.28, 43.52, 46.96, 93.28, 114.50, 116.63, 118.46, 122.40, 131.86, 147.02, 155.53, 159.40, 161.47, 163.79, 170.48. HR-MS (ESI$^+$): m/z [M + H]$^+$ calcd for $C_{20}H_{23}N_8S$, 407.1766, found 407.1814.

4-(4-Methyl-2-(methylamino)thiazol-5-yl)-2-((3-(piperidin-1-yl)phenyl)amino)pyrimidine-5-carbonitrile (12n). 12n was obtained from 1-(3-piperidine-1-yl)phenyl)guanidine and *tert*-butyl (5-(2-cyano-3-(dimethylamino)acryloyl)-4-methylthiazol-2-yl)(methyl)-carbamate. Pale yellow solid (20%); mp 254−256 °C. Anal. RP-HPLC: t_R 11.09 min (method A), 10.89 min (method C), purity 100%. ^{1}H NMR (DMSO-d_6): δ 1.48−1.58 (m, 2H, CH_2), 1.58−1.67 (m, 4H, 2 × CH_2), 2.40 (br s, 3H, CH_3), 2.89 (d, 3H, J = 4.8 Hz, CH_3), 3.14 (apparent t, 4H, J = 4.8 Hz, 2 × CH_2), 6.10−6.20 (m, 1H, Ph-H), 7.19−7.24 (m, 2H, 2 × Ph-H), 7.37 (br s, 1H, Ph-H), 8.24 (br q, 1H, J = 4.8 Hz, NH), 8.77 (s, 1H, Py-H), 10.07 (s, 1H, NH). ^{13}C NMR (DMSO-d_6): δ 19.90, 24.41, 25.69, 31.36, 50.12, 93.97, 108.55, 111.44, 111.54, 118.30, 129.31, 139.99, 152.47, 155.25, 159.45, 161.57, 163.82, 170.67. HR-MS (ESI$^+$): m/z [M + H]$^+$ calcd for $C_{21}H_{24}N_7S$, 406.1688, found 406.1871.

1-(4-(3-(5-Fluoro-4-(4-methyl-2-(methylamino)thiazol-5-yl)-pyrimidin-2-ylamino)phenyl)piperazin-1-yl)ethanone (12o). 12o was obtained from 1-(3-acetylpiperazin-1-yl)phenyl)guanidine and 3-(dimethylamino)-2-fluoro-1-(4-methyl-2-(methylamino)thiazol-5-yl)prop-2-en-1-one. Yellow solid (15%); mp 184−186 °C. Anal. RP-HPLC: t_R 11.87 min (method A), 8.90 min (method B), purity 100%. ^{1}H NMR (DMSO-d_6): δ 2.05 (s, 3H, CH_3), 2.44 (d, 3H, J = 2.8 Hz, CH_3), 2.87 (d, 3H, J = 4.8 Hz, CH_3), 3.08 (apparent t, 2H, J = 5.2 Hz, CH_2), 3.15 (apparent t, 2H, J = 5.2 Hz, CH_2), 3.53−3.62 (m, 4H, 2 × CH_2), 6.57 (dd, 1H, J = 8.0, 1.6 Hz, Ph-H), 7.12 (t, 1H, J = 8.0 Hz, Ph-H), 7.21 (d, 1H, J = 8.0 Hz, Ph-H), 7.38 (s, 1H, Ph-H), 8.10 (q, 1H, J = 4.4 Hz, NH), 8.43 (d, 1H, J = 3.6 Hz, Py-H), 9.36 (s, 1H, NH). ^{13}C NMR (DMSO-d_6): δ 19.21 (d, J = 6 Hz), 21.65, 31.31, 41.17, 45.96, 49.04, 49.48, 107.01, 109.98, 110.71 (d, J = 8 Hz), 110.87, 129.30, 141.74, 146.23 (d, J = 25 Hz), 147.23 (d, J = 12 Hz), 147.69 (d, J = 248 Hz), 151.70, 154.59, 156.47 (d, J = 2 Hz), 168.77, 171.03 (d, J = 3 Hz). HR-MS (ESI$^+$): m/z [M + H]$^+$ calcd for $C_{21}H_{25}FN_7OS$, 442.1825, found 442.1917.

5-(5-Fluoro-2-(3-(piperazin-1-yl)phenylamino)pyrimidin-4-yl)-*N*,4-dimethylthiazol-2-amine 12p. 12p was obtained from 1-(4-(3-(5-fluoro-4-(4-methyl-2-(methylamino)thiazol-5-yl)pyrimidin-2-ylamino)phenyl)piperazin-1-yl)ethanone. Yellow solid (48%); mp 134−136 °C. Anal. RP-HPLC: t_R 11.23 min (method A), 8.62 min (method B), purity 99%. ^{1}H NMR (DMSO-d_6): δ 2.44 (d, 3H, J = 3.2 Hz, CH_3), 2.81−2.90 (m, 7H, 2 × CH_2 and CH_3), 3.04 (apparent t, 4H, J = 4.8 Hz, 2 × CH_2), 6.53 (dd, 1H, J = 8.0, 1.6 Hz, Ph-H), 7.09 (t, 1H, J = 8.0 Hz, Ph-H), 7.17 (d, 1H, J = 8.0 Hz, Ph-H), 7.33 (s, 1H, Ph-H), 8.10 (br q, 1H, J = 4.8 Hz, NH), 8.43 (d, 1H, J = 3.6 Hz, Py-H), 9.32(s, 1H, NH). ^{13}C NMR (DMSO-d_6): δ 19.20 (d, J = 6 Hz), 31.31, 45.92, 49.91, 106.52, 109.54, 110.31, 110.68 (d, J = 8 Hz), 129.18, 141.65, 146.24 (d, J = 25 Hz), 147.22 (d, J = 12 Hz), 146.67 (d, J = 247 Hz), 152.49, 154.54, 156.50, 170.99. HR-MS (ESI$^+$): m/z [M + H]$^+$ calcd for $C_{19}H_{23}FN_7S$, 400.1720, found 400.1722.

5-(5-Fluoro-2-((3-morpholinophenyl)amino)pyrimidin-4-yl)-*N*,4-dimethylthiazol-2-amine 12q. 12q was obtained from 3-(dimethylamino)-2-fluoro-1-(4-methyl-2-(methylamino)thiazol-5-yl)-prop-2-en-1-one and 1-(3-morpholinophenyl)guanidine. Light pink solid (28%); mp 225−227 °C. Anal. RP-HPLC: t_R 11.89 min (method A), 11.32 min (method B), purity 98%. ^{1}H NMR (DMSO-d_6): δ 2.44 (d, 3H, J = 3.2 Hz, CH_3), 2.88 (d, 3H, J = 4.8 Hz, CH_3), 3.09 (apparent t, 4H, J = 4.8 Hz, 2 × CH_2), 3.75 (apparent t, 4H, J = 4.8 Hz, 2 × CH_2), 6.55 (dd, 1H, J = 8.0, 2.0 Hz, Ph-H), 7.12 (t, 1H, J = 8.0 Hz, Ph-H), 7.20 (dd, 1H, J = 8.0, 0.8 Hz, Ph-H), 7.36 (t, 1H, J = 2.0 Hz, Ph-H), 8.10 (q, 1H, J = 4.8 Hz, NH), 8.43 (d, 1H, J = 3.6 Hz, Py-H), 9.36 (s, 1H, NH). ^{13}C NMR (DMSO-d6): δ 19.21 (d, J = 6 Hz), 31.29, 49.23, 66.59, 106.22, 109.23, 110.68, 110.73, 129.26, 141.73, 146.23 (d, J = 25 Hz), 147.24 (d, J = 11 Hz), 147.69 (d, J = 248 Hz), 151.96, 154.57, 156.49 (d, J = 2 Hz), 170.99 (d, J = 4 Hz). HR-MS (ESI$^+$): m/z [M + H]$^+$ calcd for $C_{19}H_{22}FN_6OS$, 401.1560, found 401.1647.

5-(5-Chloro-2-((3-(piperazin-1-yl)phenyl)amino)pyrimidin-4-yl)-*N*,4-dimethylthiazol-2-amine 12r. 12r was obtained from 1-(4-(3-((5-chloro-4-(4-methyl-2-(methylamino)thiazol-5-yl)pyrimidin-2-yl)amino)phenyl)piperazin-1-yl)ethanone. Yellow solid (70%); mp 108−110 °C. Anal. RP-HPLC: t_R 11.39 min (method A), 8.75 min (method B), purity 99%. ^{1}H NMR (DMSO-d_6): δ 2.33 (s, 3H, CH_3), 2.83 (apparent t, 4H, J = 4.8 Hz, 2 × CH_2), 2.86 (d, 3H, J = 4.8 Hz, CH_3), 3.02 (apparent t, 4H, J = 5.2 Hz, 2 × CH_2), 6.55 (dd, 1H, J = 8.0, 1.2 Hz, Ph-H), 7.10 (t, 1H, J = 8.0 Hz, Ph-H), 7.16 (d, 1H, J = 8.4 Hz, Ph-H), 7.36 (s, 1H, Ph-H), 7.97 (q, 1H, J = 4.8 Hz, NH), 8.47 (s, 1H, Py-H), 9.52 (s, 1H, NH). ^{13}C NMR (DMSO-d_6): δ 19.26, 31.30, 46.10, 50.09, 106.96, 109.83, 110.60, 112.65, 116.27, 129.20, 141.17, 152.56, 153.47, 156.64, 158.14, 158.47, 170.21. HR-MS (ESI$^+$): m/z [M + H]$^+$ calcd for $C_{19}H_{23}ClN_7S$, 416.1624, found 416.1615.

1-(4-(3-((5-Chloro-4-(4-methyl-2-(methylamino)thiazol-5-yl)-pyrimidin-2-yl)amino)phenyl)piperazin-1-yl)ethanone. The compound was obtained from 2-chloro-3-(dimethylamino)-1-(4-methyl-2-(methylamino)thiazol-5-yl)prop-2-en-1-one and 1-(3-acetylpiperazin-1-yl)phenyl)guanidine. Yellow solid (42%); mp 193−195 °C. Anal. RP-HPLC: t_R 11.42 min (method C), purity 99%. ^{1}H NMR (DMSO-d_6): δ 2.05 (s, 3H, CH_3), 2.33 (s, 3H, CH_3), 2.87 (d, 3H, J = 4.4 Hz, CH_3), 3.08 (apparent t, 2H, J = 4.8 Hz, CH_2), 3.14 (apparent t, 2H, J = 4.8 Hz, CH_2), 3.53−3.62 (m, 4H, 2 × CH_2), 6.59 (dd, 1H, J = 8.0, 1.6 Hz, Ph-H), 7.13 (t, 1H, J = 8.0 Hz, Ph-H), 7.16 (dd, 1H, J = 8.0, 1.2 Hz, Ph-H), 7.40 (t, 1H, J = 2.0 Hz, Ph-H), 7.98 (q, 1H, J = 4.8 Hz, NH), 8.48 (s, 1H, Py-H), 9.56 (s, 1H, NH). ^{13}C NMR (DMSO-d_6): δ 19.30, 21.67, 31.29, 41.14, 45.92, 48.98, 49.39, 107.48, 110.32, 111.22, 112.66, 116.34, 129.35, 141.28, 151.66, 153.51, 156.64, 158.11, 158.52, 168.73, 170.20. HR-MS (ESI$^+$): m/z [M + H]$^+$ calcd for $C_{21}H_{25}ClN_7OS$, 458.1580, found 458.1157.

5-(2-((5-(1,4-Diazepan-1-yl)-2-fluorophenyl)amino)-pyrimidin-4-yl)-*N*,4-dimethylthiazol-2-amine 12s. 12s was obtained from 1-(4-(3-((5-fluoro-4-(4-methyl-2-(methylamino)thiazol-5-yl)pyrimidin-2-yl)amino)phenyl)-1,4-diazepan-1-yl)ethanone. Yellow solid (37%); mp 180−182 °C. Anal. RP-HPLC: t_R 11.19 min (method A), 10.98 min (method C), purity 100%. ^{1}H NMR (MeOH-d_4): δ 1.95−2.04 (m, 2H, CH_2), 2.48 (d, 3H, J = 2.8 Hz, CH_3), 2.88 (apparent t, 2H, J = 5.2 Hz, CH_2), 2.97 (s, 3H, CH_3), 3.07 (apparent t, 2H, J = 5.2 Hz, CH_2), 3.58−3.67 (m, 4H, 2 × CH_2), 6.43 (dd, J = 8.0, 2.0 Hz, Ph-H), 6.93 (dd, J = 8.0, 1.6 Hz, Ph-H), 7.10 (t, 1H, J = 8.0 Hz, Ph-H), 7.15 (t, 1H, J = 2.0 Hz, Ph-H), 8.24 (d, 1H, J = 3.6 Hz, Py-H). ^{13}C NMR (DMSO-d_6): δ 19.16 (d, J = 6 Hz), 29.39, 31.29, 47.72, 47.85, 48.43, 52.40, 102.42, 105.66, 106.82, 110.75, 129.46, 141.96, 146.14 (d, J = 26 Hz), 147.27 (d, J = 12 Hz), 147.65 (d, J = 248 Hz),

dx.doi.org/10.1021/jm301475f | J. Med. Chem. 2013, 56, 640−659

149.08, 154.40, 156.64, 170.98. HR-MS (ESI$^+$): m/z [M + H]$^+$ calcd for $C_{20}H_{25}FN_7S$ [M + H]$^+$, 414.1876, found, 414.1866.

2-(3-(4-Acetyl-1,4-diazepan-1-yl)phenylamino)-4-(4-methyl-2-(methylamino)thiazol-5-yl)pyrimidine-5-carbonitrile (12t). **12t** was obtained from *tert*-butyl (5-(2-cyano-3-(dimethylamino)-acryloyl)-4-methylthiazol-2-yl)(methyl)carbamate and 1-(3-(4-acetyl-1,4-diazepan-1-yl)phenyl)guanidine. Yellow solid (30%); mp 129−131 °C. Anal. RP-HPLC: t_R 12.15 min (method A), 11.55 (method C), purity 100%. ^{1}H NMR (DMSO-d_6): δ 1.76−1.92 (m, 3.6 H, CH_2 and CH_3), 1.92 (s, 1.4 H, CH_3), 2.39 (s, 3H, CH_3), 2.89 (d, 3 H, J = 4.0 Hz, CH_3), 3.28−3.34 (m, 2 H, CH_2), 3.46−3.59 (m, 6 H, 3 × CH_2), 6.48 (d, 1 H, J = 8.0 Hz, Ph-H), 7.02−7.18 (m, 3 H, 3 × Ph-H), 8.23 (q, 1H, J = 4.8 Hz, NH), 8.76 (d, 1 H, J = 0.8 Hz Py-H), 10.01 (s, 1 H, NH). ^{13}C NMR (DMSO-d_6, (*) minor rotamer): δ 19.82, 19.87*, 21.40, 21.73*, 24.42, 26.31*, 31.31, 44.33, 44.83*, 47.27, 47.35*, 47.59, 48.70*, 49.41, 50.04*, 94.00, 94.08*, 104.30, 107.50, 108.92, 118.29, 129.78, 140.42, 147.74, 148.06*, 159.49, 161.58, 161.65*, 163.78, 163.82*, 169.47, 169.71*, 170.56, 170.60*. HR-MS (ESI$^+$): m/z [M + H]$^+$ calcd for $C_{23}H_{27}N_8OS$, 463.2029, found, 463.1791.

2-(3-(1,4-Diazepan-1-yl)phenylamino)-4-(4-methyl-2-(methylamino)thiazol-5-yl)pyrimidine-5-carbonitrile (12u). **12u** was obtained from 2-(3-(4-acetyl-1,4-diazepan-1-yl)phenylamino)-4-(4-methyl-2-(methylamino)thiazol-5-yl)pyrimidine-5-carbonitrile. Yellow solid (34%); mp 210−212 °C. Anal. RP-HPLC: t_R 11.19 min (method A), 10.94 min (method C), purity 100%. ^{1}H NMR (DMSO-d_6): δ 1.79−1.92 (m, 2H, CH_2), 2.40 (s, 3H, CH_3), 2.77 (apparent t, 2H, J = 5.2 Hz, CH_2), 2.89 (d, 3H, J = 4.0 Hz, CH_3), 2.97 (apparent t, 4H, J = 4.8 Hz, CH_2), 3.53 (apparent t, 4H, J = 5.2 Hz, 2 × CH_2), 6.45 (dd, 1H, J = 8.0, 2.0 Hz, Ph-H), 6.99−7.15 (m, 3H, 3 × Ph-H), 8.24 (br q, 1H, J = 5.2 Hz, NH), 8.76 (s, 1H, Py-H), 10.01 (s, 1H, NH). ^{13}C NMR (DMSO-d_6): δ 19.87, 28.10, 31.31, 47.06, 47.65, 50.51, 93.97, 104.21, 107.41, 108.70, 115.00, 118.31, 129.65, 140.35, 148.98, 154.98, 159.50, 161.61, 163.80, 170.57. HR-MS calcd for $C_{21}H_{25}N_8S$, 419.1878, found, 419.1862.

1-(4-(Bromomethyl)-2-(methylamino)thiazol-5-yl)ethanone (13). To an ice-cooled solution of 1-(4-methyl-2-(methylamino)-thiazol-5-yl)ethanone (3.4 g, 20.0 mmol) in 50 mL of $CHCl_3$ was added *N*-bromosuccinimide (3.5 g, 20.0 mmol). After being stirred at room temperature for 3 h, the mixture was washed with saturated aqueous $NaHCO_3$, and the organic layer was dried over $MgSO_4$, filtered, and concentrated. The precipitates were collected and washed with MeOH to afford the title compound as a white solid (2.76 g, 56%), mp 149 °C (dec). ^{1}H NMR (DMSO-d_6): δ 2.41 (s, 3H, CH_3), 2.87 (d, 3H, J = 4.8 Hz, CH_3), 4.74 (s, 2H, CH_2), 8.57 (d, H, J = 4.4 Hz, NH). HR-MS (ESI$^+$): m/z [M + H]$^+$ calcd for $C_7H_{10}BrN_2OS$, 250.9677, found 250.9607. *tert*-Butyl 5-acetyl-4-(bromomethyl)thiazol-2-yl(methyl)carbamate was obtained by reacting **13** and di-*tert*-butyl dicarbonate as white solid (98%), mp 84−86 °C. ^{1}H NMR ($CDCl_3$): δ 1.61 (s, 9H, 3 × CH_3), 2.54 (s, 3H, CH_3), 3.60 (s, 3H, CH_3), 5.34 (s, 2H, CH_2). HR-MS (ESI$^+$): m/z [M + H]$^+$ calcd for $C_{12}H_{18}Br\ N_2O_3S$, 351.0210, found 351.0338.

***tert*-Butyl 5-Acetyl-4-(2,2,2-trifluoroethyl)thiazol-2-yl-(methyl)carbamate (14).** A solution of *tert*-butyl 5-acetyl-4-(bromomethyl)thiazol-2-yl(methyl)carbamate (8.45 g, 24.0 mmol) in DMF was treated with methyl 2,2-difluoro-2-(fluorosulfonyl)acetate (5.7 mL, 45.0 mmol) and CuI (2.9 g, 15.0 mmol). The mixture was heated at 80 °C for 12 h. After completion of the reaction, the mixture was purified by chromatography using EtoAc/PE to afford the title compound as a white solid (4.13g, 51%), mp 93−95 °C. ^{1}H NMR ($CDCl_3$): δ 1.61 (s, 9H, 3 × CH_3), 2.53 (s, 3H, CH_3), 3.59 (s, 3H, CH_3), 4.03 (q, 2H, J = 10.4 Hz, CH_2). ^{13}C NMR ($CDCl_3$): δ 28.10, 30.84, 34.12, 35.00 (q, J = 30 Hz), 84.36, 124.15 (q, J = 276 Hz), 127.96, 146.63 (q, J = 3 Hz), 153.26, 161.96. 190.21. HRMS (ESI$^+$): m/z [M + H]$^+$ calcd for $C_{13}H_{18}F_3N_2O_3S$, 339.0990, found 339.1058.

***tert*-Butyl 5-(3-(Dimethylamino)acryloyl)-4-(2,2,2-trifluoroethyl)thiazol-2-yl(methyl)carbamate (15, R^1 = Boc, R′ = CH_2CF_3).** **15** (R^1 = Boc, R′ = CH_2CF_3) was obtained from *tert*-butyl 5-acetyl-4-(2,2,2-trifluoroethyl)thiazol-2-yl(methyl)carbamate and DMF−DMA. Light yellow solid (69%); mp 150−152 °C. ^{1}H NMR (DMSO-d_6): δ 1.54 (s, 9H, 3 × CH_3), 2.89 (s, 3H, CH_3), 3.15 (s, 3H, CH_3), 3.46 (s, 3H, CH_3), 4.19 (q, 2H, J = 11.2 Hz, CH_2), 5.31 (d, 1H, J = 12.0 Hz, CH), 7.71 (d, 1H, J = 12.0 Hz, CH). ^{13}C NMR ($CDCl_3$): δ 28.16, 34.01, 34.78 (q, J = 30 Hz), 37.45, 45.12, 83.66, 95.10, 125.60 (q, J = 273 Hz), 129.99, 143.94 (q, J = 3 Hz), 153.38, 153.72, 160.06, 180.77. HR-MS (ESI$^+$): m/z [M + H]$^+$ calcd for $C_{16}H_{23}F_3N_3O_3S$, 394.1412, found 394.1359.

***tert*-Butyl (5-(3-(Dimethylamino)acryloyl)-4-(trifluoromethyl)thiazol-2-yl)(methyl)car bamate (15, R^1 = Boc, R′ = CF_3).** **15** (R^1 = Boc, R′ = CF_3) was obtained from *tert*-butyl (5-acetyl-4-(trifluoromethyl)thiazol-2-yl)(methyl)carbamate and DMF−DMA. Orange solid (77%); mp 116−118 °C. ^{1}H NMR ($CDCl_3$): δ 1.61 (s, 9H, 3 × CH_3), 2.91 (s, 3H, CH_3), 3.16 (s, 3H, CH_3), 3.57 (s, 3H, CH_3), 5.44 (d, 2H, J = 12.4 Hz, CH), 7.70 (d, 1H, J = 12.4 Hz, CH). HR-MS (ESI$^+$): m/z [M + H]$^+$ calcd for $C_{15}H_{21}F_3N_3O_3S$, 380.1256, found 380.1038.

***tert*-Butyl (5-(3-(Dimethylamino)acryloyl)thiazol-2-yl)-(methyl)carbamate (15, R^1 = Boc, R′ = H).** **15** (R^1 = Boc, R′ = H) was obtained from *tert*-butyl (5-acetylthiazol-2-yl)(methyl)-carbamate and DMF−DMA. Yellow solid (92%); mp 170−172 °C. ^{1}H NMR ($CDCl_3$): δ 1.61 (s, 9H, 3 × CH_3), 2.92 (brs, 3H, CH_3), 3.14 (brs, 3H, CH_3), 3.57 (s, 3H, CH_3), 5.48 (d, 2H, J = 12.4 Hz, CH), 7.77 (d, 1H, J = 12.4 Hz, CH), 7.95 (s, 1H, CH). ^{13}C NMR ($CDCl_3$): δ 28.18, 34.04, 37.45, 44.99, 83.76, 92.58, 135.91, 139.87, 152.94, 153.16, 164.20, 180.55. HR-MS (ESI$^+$): m/z [M + H]$^+$ calcd for $C_{14}H_{22}N_3O_3S$, 312.1382, found 312.1168.

***tert*-Butyl (4-Cyclopropyl-5-(3-(dimethylamino)acryloyl)-thiazol-yl)(methyl)carbamate (15, R^1 = Boc, R′ = cycloprop).** **15** (R^1 = Boc, R′ = cycloprop) was obtained from *tert*-butyl (5-acetyl-4-cyclopropylthiazol-2-yl)(methyl)carbamate and DMF−DMA. Orange solid (61%); mp 151−153 °C. ^{1}H NMR ($CDCl_3$): δ 0.89−0.97 (m, 4H, 2 × CH_2), 1.52 (s, 9H, 3 × CH_3), 2.86 (bs, 3H, CH_3), 2.94−3.02 (m, 1H, CH), 3.13 (br s, 3H, CH_3), 3.35 (s, 3H, CH_3), 5.35 (d, 1H, J = 12.0 Hz, CH), 7.64 (d, 1H, J = 12.4 Hz. CH). ^{13}C NMR ($CDCl_3$): δ 9.30, 11.93, 28.19, 33.77, 37.35, 45.00, 83.31, 95.77, 126.02, 152.85, 153.27, 157.99, 160.12, 182.16. HRMS (ESI$^+$): m/z [M + H]$^+$ calcd for $C_{17}H_{26}N_3O_3S$, 352.1695, found 352.1647.

***tert*-Butyl (5-(3-(Dimethylamino)acryloyl)-4-phenylthiazol-2-yl)(methyl)carbamate (15, R^1 = Boc, R′ = Ph).** **15** (R^1 = Boc, R′ = Ph) was obtained from *tert*-butyl (5-acetyl-4-phenylthiazol-2-yl)-(methyl)carbamate and DMF−DMA. Yellow solid (66%); mp 166−167 °C. ^{1}H NMR ($CDCl_3$): δ 1.61 (s, 9H, 3 × CH_3), 2.53 (br s, 3H, CH_3), 3.02 (br s, 3H, CH_3), 3.58 (s, 3H, CH_3), 5.11 (d, 1H, J = 12.4 Hz, CH), 7.32−7.43 (m, 3H, 3 × Ph-H), 7.58 (d, 1H, J = 12.4 Hz, CH), 7.64−7.72 (m, 2H, 2 × Ph-H). ^{13}C NMR ($CDCl_3$): δ 28.22, 33.92, 36.88, 44.89, 83.62, 95.71, 127.91, 128.34, 129.86, 131.15, 136.16, 150.34, 152.91, 153.10, 161.23, 182.16. HR-MS (ESI$^+$): m/z [M + H]$^+$ calcd for $C_{20}H_{26}N_3O_3S$ [M + H]$^+$, 388.1695, found, 388.1595. *tert*-Butyl (5-acetyl-4-phenylthiazol-2-yl)(methyl)carbamate was obtained from 1-(2-(methylamino)-4-phenylthiazol-5-yl)ethanone and di-*tert*-butyl dicarbonate. Colorless liquid (81%). ^{1}H NMR ($CDCl_3$): δ 1.62 (s, 9H, 3 × CH3), 2.20 (s, 3H, CH3), 3.59 (s, 3H, CH3), 7.43−7.50 (m, 3H, 3 × Ph-H), 7.56−7.65 (m, 3H, 2 × Ph-H). HRMS (ESI$^+$): m/z [M + H]$^+$ calcd for $C_{17}H_{21}N_2O_3S$ [M + H]$^+$, 333.1273, found, 333.1247.

1-(2-(Methylamino)-4-(trifluoromethyl)thiazol-5-yl)-ethanone (16). To a solution of 1,1,1-trifluoropentane-2,4-dione (1.0 g, 6.4 mmol) in 15 mL of acetonitrile was added hydroxy(tosyloxy)-iodobenzene (3.0 g, 7.7 mmol), and the mixture was refluxed for 1 h. When the mixture was cooled, 1-methylthiourea (0.69 g, 7.7 mmol) was added and the mixture was heated under reflux for 4 h. The mixture was concentrated and purified using PE/EtOAc as eluant to yield the title compound as a white solid (2.66 g, 53%), mp 133−135 °C. ^{1}H NMR (DMSO-d_6) δ: 2.42 (d, 3H, J = 0.8 Hz, CH_3), 2.88 (d, 3H, J = 4.8 Hz, CH_3), 8.86 (bs, 1H, NH). ^{13}C NMR (DMSO-d_6): δ 29.87 (d, J = 3 Hz), 31.59, 120.44 (q, J = 271 Hz), 125.57, 141.93 (q, J = 36 Hz), 171.05, 187.48. HR-MS (ESI$^+$): m/z [M + H]$^+$ calcd for $C_7H_8\ F_3N_2OS$, 225.0309, found 225.0309.

***tert*-Butyl (5-Acetyl-4-(trifluoromethyl)thiazol-2-yl)(methyl)-carbamate (17).** **17** was obtained from 1-(2-(methylamino)-4-(trifluoromethyl)thiazol-5-yl)ethanone and di-*tert*-butyl dicarbonate.

dx.doi.org/10.1021/jm301475f | J. Med. Chem. 2013, 56, 640−659

White solid (94%). ^{1}H NMR ($CDCl_3$): δ 1.62 (s, 9H, 3 × CH_3), 2.60 (d, 3H, J = 0.8 Hz, CH_3), 3.59 (s, 3H, CH_3). HR-MS (ESI$^+$): m/z [M − (*tert*-butyl) + H]$^+$ calcd for $C_8H_8F_3N_2O_3S$, 269.0208, found 269.0265.

***N*,*N*-Dimethyl-*N*′-(methylcarbamothioyl)formimidamide (18).** A mixture of *N*-methylthiourea (9.0 g, 100 mmol) and DMF−DMA (12 mL, 120 mmol) in 50 mL of $CHCl_3$ was refluxed overnight. The mixture was concentrated and the resulting precipitate was collected by filtration to afford **18** as white solid (14.3 g, 98%), mp 109−110 °C. ^{1}H NMR ($CDCl_3$): δ 3.02 (d, 0.9H, J = 5.2 Hz, CH_3), 3.04 (s, 2.1H, CH_3), 3.13 (s, 0.9H, CH_3), 3.15 (s, 2.1H, CH_3), 3.19 (s, 0.9H, CH_3), 3.21 (d, 2.1H, J = 5.2 Hz, CH_3), 6.88 (brs, 1H, NH), 8.85 (s, 0.3H, CH), 8.88 (s, 0.7H, CH). HR-MS (ESI$^+$): m/z [M + H]$^+$ calcd for $C_5H_{12}N_3S$, 146.0752; found 146.0638.

1-(2-(Methylamino)thiazol-5-yl)ethanone (19). A mixture of *N*,*N*-dimethyl-*N*′-(methylcarbamothioyl)formimidamide (3.62 g, 25.0 mmol) and chloroacetone chloride (2 mL, 25.0 mmol) in 50 mL of acetonitrile was refluxed for 4 h. After completion of the reaction, the mixture was concentrated, neutralized by saturated $NaHCO_3$ solution, and dried over air to yield the title compound as a white solid (3.10 g, 79%), mp 163−164 °C. ^{1}H NMR (DMSO-d_6): δ 2.35 (s, 3H, CH_3), 2.88 (s, 3H, CH_3), 8.00 (s, H, thiazol-H), 8.54 (br s, 1H, NH). ^{13}C NMR (DMSO-d_6): δ 26.03, 31.55, 127.66, 150.04, 175.29, 188.75. HR-MS (ESI$^+$): m/z [M + H]$^+$ calcd for $C_6H_9N_2OS$, 157.0436; found 157.0269.

***tert*-Butyl (5-Acetylthiazol-2-yl)(methyl)carbamate (20).** **20** was obtained from 1-(2-(methylamino)thiazol-5-yl)ethanone and di-*tert*-butyl dicarbonate. White solid (95%). ^{1}H NMR ($CDCl_3$): δ 1.61 (s, 9H, 3 × CH_3), 2.53 (s, 3H, CH_3), 3.59 (s, 3H, CH_3), 8.00 (s, 1H, thiazol-H). HR-MS (ESI$^+$): m/z [M + H]$^+$ calcd for $C_{11}H_{17}N_2O_3S$, 257.0960; found 257.0994.

***tert*-Butyl (4-Cyclopropylthiazol-2-yl)(methyl)carbamate (23).** A solution of 1-cyclopropylethanone (8.41 g, 100 mmol) in 30 mL of methanol was cooled in an ice bath, and bromine (5.15 mL, 100 mmol) was added dropwise. The mixture was stirred for 1 h before being warmed to room temperature. After the mixture was stirred for a further 3 h, 50 mL of water was added. The mixture was extracted by diethyl ether (3 × 100 mL) and the combined organic phase was washed with brine, dried over $MgSO_4$, and concentrated to yield **22** as a colorless oil (12.49 g, 77%). ^{1}H NMR ($CDCl_3$): δ 0.98−1.04 (m, 2H, CH_2), 1.08−1.14 (m, 2H, CH_2), 2.14−2.23 (m, 1H, CH), 4.02 (s, 2H, CH_2). A solution of **22** (12.49 g, 76.0 mmol) in 30 mL of methanol was treated with 1-methylthiourea (6.84 g, 76.0 mmol), and an amount of 2 mL of pyridine was added. After being stirred at room temperature overnight, the mixture was concentrated and basified with saturated $NaHCO_3$ solution. The precipitate was filtered and dried over air. 4-Cyclopropyl-*N*-methylthiazol-2-amine was obtained as a white solid after recrystallization from PE/EtOAc (5.70 g, 49%). ^{1}H NMR ($CDCl_3$): δ 0.76−0.81 (m, 2H, CH_2), 0.81−0.87 (m, 2H, CH_2), 1.81−1.90 (m, 1H, CH), 2.95 (s, 3H, CH_3), 5.46 (br s, 1H, NH), 7.07 (s, 1H, thiazol-H). HR-MS (ESI$^+$): m/z [M + H]$^+$ calcd for $C_7H_{11}N_2S$, 155.0643; found 155.0452. The latter was treated with di-*tert*-butyl dicarbonate to afford the title compound **23** as a brown liquid (55%). ^{1}H NMR ($CDCl_3$) δ: 0.81−0.90 (m, 4H, 2 × CH_2), 1.58 (s, 9H, 3 × CH_3), 1.89−1.99 (m, 1H, CH), 3.52 (s, 3H, CH_3), 6.45 (s, 1H, thiazol-H). HR-MS (ESI$^+$): m/z [M + H]$^+$ calcd for $C_{12}H_{19}N_2O_2S$, 255.1167; found 255.1184.

***tert*-Butyl (5-Acetyl-4-cyclopropylthiazol-2-yl)(methyl)-carbamate (24).** A solution of **23** (3.81g, 15.0 mmol) in 20 mL of anhydrous THF at −78 °C was treated with 25.0 mmol of LDA. After the mixture was stirred for 30 min, acetaldehyde (20.0 mmol, 1.12 mL) was added and the reaction was continued for 2 h. After completion of the reaction, 20 mL of water was added and the mixture was treated with 2 M aqueous HCl solution. After concentration, the mixture was extracted with $CHCl_3$ (3 × 50 mL). The combined organic phase was washed with brine, dried over $MgSO_4$, filtered, and concentrated to dryness. The resulting mixture was dissolved in 30 mL of $CHCl_3$ and then treated with MnO_2 (10 equiv). The mixture was heated under reflux for 4 h. The reaction mixture was purified using PE/EtOAc as elutant to afford the title compound as a yellow solid (3.51 g, 79%), mp 89−90 °C. ^{1}H NMR ($CDCl_3$): δ 0.98−1.08 (m, 2H, CH_2), 1.09−1.18 (m, 2H, CH_2), 1.60 (s, 9H, 3 × CH_3), 2.51 (s, 3H, CH_3), 2.98−3.10 (m, 1H, CH), 3.49 (s, 3H, CH_3). ^{13}C NMR (DMSO-d_6): δ 10.12, 12.10, 28.14, 30.92, 33.86, 83.95, 124.81, 153.15, 161.43, 162.18, 190.96. HR-MS (ESI$^+$): m/z [M + H]$^+$ calcd for $C_{14}H_{21}N_2O_3S$, 297.1273, found 297.1296.

1-(2-(Methylamino)-4-phenylthiazol-5-yl)ethanone (26). To a solution of *N*-methyl-4-phenylthiazol-2-amine (1.90 g, 10 mmol) and anhydrous $AlCl_3$ (6.7 g, 50 mmol) in 100 mL of CH_2Cl_2 under nitrogen gas was added acetyl chloride (1.42 mL, 20 mmol) over 15 min. The reaction was continued for 2 h. The mixture was cooled in an ice bath and quenched using MeOH. After being concentrated, the mixture was purified by column chromatography using EtOAc/PE as eluant to affort the title compound as a white solid (1.55g, 67%), mp 229−231 °C. ^{1}H NMR (DMSO-d_6): δ 1.90 (s, 1H, CH3), 2.88 (d, 1H, J = 4.8 Hz, CH_3), 7.42−7.50 (m, 3H, 3 × Ph-H), 7.50−7.56 (m, 2H, 2 × Ph-H), 8.52 (br q, 1H, J = 4.8 Hz, NH). ^{13}C NMR (DMSO-d_6): δ 28.64, 31.40, 124.06, 128.53, 129.49, 129.80, 136.19, 159.09, 171.46, 189.10. HR-MS: m/z [M + H]$^+$ calcd for $C_{12}H_{13}N_2OS$, 233.0749, found, 233.0658. *N*-Methyl-4-phenylthiazol-2-amine was obtained from benzoyl chloride and 1-methylthiourea as a white solid (100%), mp 143−144 °C. ^{1}H NMR (DMSO-d_6): δ 2.99 (s, 3H, CH_3), 7.18 (s, 1H, thiazol-H), 7.36−7.43 (m, 1H, Ph-H), 7.43−7.50 (m, 2H, 2 × Ph-H), 7.75−7.81 (m, 2H, 2 × Ph-H), 8.73 (br s, 1H, NH). HRMS: m/z [M + H]$^+$ calcd for $C_{10}H_{11}N_2S$, 191.0643; found 191.0512.

***N*-Methyl-5-(2-(3-nitrophenylamino)pyrimidin-4-yl)-4-phenylthiazol-2-amine (27a).** **27a** was obtained from 1-(3-nitrophenyl)guanidine and *tert*-butyl (5-(3-(dimethylamino)acryloyl)-4-phenylthiazol-2-yl)(methyl)carbamate. Yellow solid (18%); mp 215−216 °C. Anal. RP-HPLC: t_R 13.84 min (method A), 13.45 min (method B), purity 97%. ^{1}H NMR (DMSO-d_6): δ 2.92 (d, 3H, J = 4.8 Hz, CH_3), 6.33 (d, 1H, J = 5.2 Hz, Py-H), 7.40−7.60 (m, 6H, 6 × Ph-H), 7.76−7.84 (m, 1H, Ph-H), 7.97−8.06 (m, 1H, Ph-H), 8.16 (d, 1H, J = 5.6 Hz, Py-H), 8.27 (q, 1H, J = 4.8 Hz, NH), 8.98 (t, 1H, J = 3.0 Hz, Ph-H), 10.05 (s, 1H, NH). ^{13}C NMR (DMSO-d_6): δ 31.49, 107.90, 112.77, 115.97, 119.41, 125.04, 129.12, 129.37, 130.09, 136.47, 142.37, 148.65, 154.89, 157.58, 159.21, 159.57, 170.52. HR-MS: m/z [M + H]$^+$ calcd for $C_{20}H_{17}N_6O_2S$, 405.1134; found, 405.1118.

***N*-Methyl-5-(2-((3-nitrophenyl)amino)pyrimidin-4-yl)-4-(2,2,2-trifluoroethyl)thiazol-2-amine (27b).** **27b** was obtained from 1-(3-nitrophenyl)guanidine and *tert*-butyl 5-(3-(dimethylamino)-acryloyl)-4-(2,2,2-trifluoroethyl)thiazol-2-yl(methyl)carbamate. Yellow solid (47%); mp 265−267 °C. Anal. RP-HPLC: t_R 13.94 min (method A), 11.85 min (method B), purity 99%. ^{1}H NMR (DMSO-d_6): δ 2.89 (d, 3H, J = 4.4 Hz, CH_3), 4.11 (q, 2H, J = 11.2 Hz, CH_2), 7.01 (d, 2H, J = 5.2 Hz, Py-H), 7.58 (t, 1H, J = 8.0 Hz, Ph-H), 7.78−7.85 (m, 1H, Ph-H), 8.05 (dd, 1H, J = 5.2, 1.6 Hz, Ph-H), 8.33 (q, 1H, J = 4.8 Hz, NH), 8.48 (d, 1H, J = 5.6 Hz, Py-H), 8.59 (t, 1H, J = 2.0 Hz, Ph-H), 10.07 (s, 1H, NH). ^{13}C NMR (DMSO-d_6): δ 31.52, 35.33 (q, J = 29 Hz), 109.05, 113.11, 116.22, 121.42, 126.21 (q, J = 276 Hz), 125.34, 130.18, 142.18, 144.49, 148.60, 158.26, 159.03, 159.45, 170.07. HR-MS (ESI$^+$): m/z [M + H]$^+$ calcd for $C_{16}H_{14}F_3N_6O_2S$, 411.0851, found 411.1019.

3-((4-(2-(Methylamino)-4-(trifluoromethyl)thiazol-5-yl)-pyrimidin-2-yl)amino)benzenesulfonamide (27f). **27f** was obtained from *tert*-butyl (5-(3-(dimethylamino)acryloyl)-4-(trifluoromethyl)thiazol-2-yl)(methyl)carbamate and 3-guanidinobenzenesulfonamide. Yellow solid (10%); mp 279−281 °C. Anal. RP-HPLC: t_R 13.00 min (method A), 11.32 (method B), purity 100%. ^{1}H NMR (DMSO-d_6): δ 2.91 (d, 3H, J = 4.8 Hz, CH_3), 7.03 (dt, 1H, J = 5.2, 1.2 Hz, Py-H), 7.31 (s, 2H, NH_2), 7.44 (dt, 1H, J = 8.0, 1.2 Hz, Ph-H), 7.49 (t, 1H, J = 8.0 Hz, Ph-H), 7.88 (d, 1H, J = 8.0 Hz, Ph-H), 8.39 (s, 1H, Ph-H), 8.50 (q, 1H, J = 4.8 Hz, NH), 8.56 (d, 1H, J = 5.2 Hz, Py-H), 10.05 (s, 1H, NH). ^{13}C NMR (DMSO-d_6): δ 31.63, 109.34, 116.19, 119.18, 121.28 (q, J = 276 Hz), 122.27, 125.72, 129.54, 137.80 (q, J = 35 Hz), 141.04, 145.03, 156.11, 159.63, 159.74, 170.54. HR-MS (ESI$^+$): m/z [M + H]$^+$ calcd for $C_{15}H_{14}F_3N_6O_2S_2$, 431.0572, found 431.0766.

dx.doi.org/10.1021/jm301475f | J. Med. Chem. 2013, 56, 640−659

3-((4-(2-(Methylamino)thiazol-5-yl)pyrimidin-2-yl)amino)-benzenesulfonamide (27i). **27i** was obtained from *tert*-butyl (5-(3-(dimethylamino)acryloyl)thiazol-2-yl)(methyl)carbamate and 3-guanidinobenzenesulfonamide. Yellow solid (13%); mp 295−297 °C. Anal. RP-HPLC: t_R 11.09 min (method A), 8.72 (method B), purity 99%. ^{1}H NMR (DMSO-d_6): δ 2.90 (d, 3H, J = 4.8 Hz, CH_3), 7.19 (d, 1H, J = 5.2 Hz, Py-H), 7.29 (s, 2H, NH_2), 7.44 (dt, 1H, J = 8.0, 1.6 Hz, Ph-H), 7.46 (t, 1H, J = 8.0 Hz, Ph-H), 7.88−7.95 (m, 1H, Ph-H), 8.08 (s, 1H, thiazol-H), 8.20 (q, 1H, J = 4.8 Hz, NH), 8.34 (d, 1H, J = 5.2 Hz, Py-H), 8.43 (t, 1H, J = 1.6 Hz, Ph-H), 9.81 (s, 1H, NH). ^{13}C NMR (DMSO- d_6): δ 31.50, 106.60, 116.00, 118.66, 121.92, 124.27, 129.44, 141.55, 143.64, 144.96, 157.64, 159.07, 159.97, 173.00. HR-MS (ESI$^+$): m/z [M + H]$^+$ calcd for $C_{14}H_{15}N_6O_2S_2$, 363.0698, found 363.0666.

3-((4-(4-Cyclopropyl-2-(methylamino)thiazol-5-yl)pyrimidin-2-yl)amino)benzenesulfonamide (27j). **27j** was obtained from *tert*-butyl (4-cyclopropyl-5-(3-(dimethylamino)acryloyl)thiazol-2-yl)-(methyl)carbamate and 3-guanidinobenzenesulfonamide. Off-white solid (15%); mp 258−260 °C. Anal. RP-HPLC: t_R 11.55 min (method A), 9.22 min (method B), purity 100%. ^{1}H NMR (DMSO-d_6): δ 0.93−1.04 (m, 4H, 2 × CH_2), 2.52−2.62 (m, 1H, CH), 2.83 (d, 1H, J = 4.8 Hz, CH_3), 7.09 (d, 1H, J = 5.6 Hz, Py-H), 7.28 (s, 2H, NH_2), 7.40 (d, 1H, J = 8.0 Hz, Ph-H), 7.46 (t, 1H, J = 8.0 Hz, Ph-H), 7.96 (d, 1H, J = 8.0 Hz, Ph-H), 8.05 (q, 1H, J = 4.8 Hz, NH), 8.33 (s, 1H, Ph-H), 8.36 (d, 1H, J = 5.2 Hz, Py-H), 9.75 (s, 1H, NH). ^{13}C NMR (DMSO-d_6): δ 9.27, 13.07, 31.46, 108.32, 116.08, 117.37, 118.67, 122.04, 129.41, 141.56, 144.97, 158.08, 158.50, 159.41, 159.73, 170.37. HR-MS (ESI$^+$): m/z [M + H]$^+$ calcd for $C_{17}H_{19}N_6O_2S_2$, 403.1011, found 403.0900.

Crystallography. CDK9$_{330}$ (residues 1−330)/cyclin T1 (residues 1−259, Q77R, E96G, F241L) compounds were expressed, purified, and crystallized as described previously.[51] Crystals were grown by vapor diffusion against a reservoir containing 14% PEG1000, 100 mM sodium potassium phosphate, pH 6.2, 500 mM NaCl, 4 mM TCEP. A crystal was soaked in mother liquor containing also 1 mM **12u** and 15% glycerol for 45 min before cryocooling in liquid nitrogen.

CDK2/cyclin A was expressed and purified as described previously.[57] Purified protein was incubated with **12u**, filtered, and cocrystallized in 1.25 M ammonium sulfate, 0.5 M potassium chloride, 100 mM Hepes, pH 7.0, 5 mM DTT at 4 °C. Crystals were cryoprotected and frozen in 7 M sodium formate in the presence of 1 mM **12u**.

Diffraction data for the CDK9/cyclin T1/**12u** and CDK2/cyclin A/**12u** were collected from single crystals at Diamond Light Source beamline I03. Diffraction data for CDK9/cyclin T/**12u** were processed with XDS[58] and SCALA (CCP4).[59] PHENIX.refine[60] was used for rigid body refinement with a model derived from 3BLH as the initial model. REFMAC[61] was used for subsequent TLS and restrained refinement. Jelly body restraints to an external model (3BLH) were used during refinement. CDK2/cyclin A data were processed using XDS[58] and SCALA.[59] Molecular replacement was performed by the program PHASER[62] using a search model derived from PDB entry 3DDQ. Ligand restraints were defined using PHENIX, and structures were refined and rebuilt using PHENIX.refine and COOT.[63]

Kinase Assay. Inhibition of CDKs and other kinases was measured by radiometric assay Millipore's KinaseProfiler according to the protocols detailed at http://www.millipore.com/drugdiscovery/dd3/, where ATP concentration for each specific kinase assay was set within 15 μM of the apparent K_m for ATP where determined. Half-maximal inhibition (IC_{50}) values were calculated from 10-point dose−response curves, and apparent inhibition constants (K_i) were calculated from the IC_{50} values and K_m (ATP) values for the kinases in question as described.[35] The assay details can also be found in the Supporting Information.

Cell Culture. All cancer cell lines were obtained from the cell bank at the Centre for Biomolecular Sciences, University of Nottingham, U.K. The HMEC-1 cell line was purchased (ECACC), and cells were cultured in essential medium with 10% fetal bovine serum (FBS), 7.5% sodium bicarbonate, 1% 0.1 mM nonessential amino acids, 1% 1 M HEPES, 1% 200 mM L-glutamine, and 1% penicillin. Other cell lines were maintained in RPMI-1640 with 10% FBS.

Proliferation Assays. MTT (3-(4,5-dimethylthiazol-2-yl)-2,5-diphenyltetrazolium bromide, Sigma) assays were performed as reported previously.[35] Compound concentrations required to inhibit 50% of cell growth (GI_{50}) were calculated using nonlinear regression analysis.

Caspase-3/7 Assay. Activity of caspase 3/7 was measured using the Apo-ONE homogeneous caspase-3/7 kit (Promega G7790).[18]

Cell Cycle Analysis and Detection of Apoptosis. Cells (4× 10^5) were cultured for 48 h in medium alone or with varying concentrations of inhibitor. Cell cycle status was analyzed using a Beckman Coulter EPICS-XL MCL flow cytometer, and data were analyzed using EXPO32 software. Apoptosis was also confirmed using FITC annexin V/PI (propidium idodide) staining after cells were cultured in medium only or with varying concentrations of inhibitors according to the protocols (BD Bioscience). The annexin V/PI-positive apoptotic cells were enumerated using flow cytometry. The percentage of cells undergoing apoptosis was defined as the sum of early apoptosis (annexin V-positive cells) and late apoptosis (annexin V-positive and PI-positive cells). The pan-caspase inhibitor Z-Val-Ala-Asp-(OMe)-CH_2F (Z-VAD-fmk, Sigma) was dissolved in DMSO and used at 25 μM.

Detection of Apoptosis in Primary CLL Cells. Freshly isolated primary CLL cells and normal B- and T-cells were cultured in RPMI with 10% fetal calf serum and L-glutamine, penicillin, and streptomycin. Cells were maintained at 37 °C in an atmosphere containing 95% air and 5% CO_2 (v/v). CLL cells (10^6/mL) were treated with inhibitor for 48 h. Subsequently, cells were labeled with CD19-APC (Caltag) and then resuspended in 200 μL of binding buffer containing 4 μL of annexin V-FITC (Bender Medsystems, Vienna, Austria). Apoptosis was quantified in the CD19$^+$ CLL cells, CD19$^+$ normal B-cells, and CD3$^+$ normal T-cells using an Accuri C6 flow cytometer and FlowJo software (TreeStar). LD_{50} values were calculated from line-of-best-fit analysis of the sigmoidal dose−response curves.

Western Blots. Western blotting was performed as described.[20] Antibodies used were as follows: total RNAP-II (8WG16), phosphorylated RNAP-II Ser-2 (Covance), Bcl-2 (Dako, Denmark A/S), MDM2 and β-actin (Sigma-Aldrich), Mcl-1, PARP (Cell Signaling Technology). Both anti-mouse and anti-rabbit immunoglobulin G (IgG) horseradish peroxidase-conjugated antibodies were obtained from Dako.

Statistical Analysis. All experiments were performed in triplicate and repeated at least twice, representative experiments being selected for figures. Statistical significance of differences for experiments was determined using one-way analysis of variance (ANOVA), with a minimal level of significance at $p < 0.01$.

■ ASSOCIATED CONTENT

Ⓢ Supporting Information

Synthesis and characterization of compounds **Ic**, **27c−e**, **27g**,-**h**, and **27k**,**l**, and kinase assays. This material is available free of charge via the Internet at http://pubs.acs.org.

Accession Codes

PDB codes are the following: CDK9/cyclin T/**12u**, 4BCG; CDK2/cyclin A/**12u**, 4BCP.

■ AUTHOR INFORMATION

Corresponding Author

*Phone: +61883022372. E-mail: shudong.wang@unisa.edu.au.

Author Contributions

Overall research design and writing of the manuscript: Wang. Chemistry experiments: Shao, Shi, Huang, and Foley. Biological experiments: Abbas, Liu, and Lam. Ex vivo CLL experiments: Pepper. Crystallographic experiments: Hole, Noble, Endicott,

and Baumli. Contributions to or assistance in preparation of the manuscript: Shao, Pepper, Hole, Noble, Endicott, and Fischer.

Notes

The authors declare no competing financial interest.

■ ACKNOWLEDGMENTS

This study was supported by Cancer Research UK Grants C21568/A8988 and C21568/A12474.

■ ABBREVIATIONS USED

ATP, adenosine triphosphate; Bcl-2, B-cell lymphoma 2; CaMK1, calcium/calmodulin-dependent protein kinase type 1; DCM, dichloromethane; DMF, *N*,*N*-dimethylformamide; DMSO, dimethylsulfoxide; DTT, dithiothreiol; HRMS, high resolution mass spectrometry; IKKβ, inhibitor of nuclear factor κB kinase subunit β; Lck, lymphocyte-specific protein tyrosine kinase; LDA, lithium diisopropylamide; MeCN, acetonitrile; MAPK2, mitogen-activated protein kinase 2; Mcl-1, myeloid cell leukemia sequence 1; NBS, *N*-bromosuccinimide; NCS, *N*-chlorosuccinimide; PDB, Protein Data Bank; PARP, poly ADP-ribose polymerase; PKA, protein kinase A; PKB, protein kinase B; PKC, protein kinase C; RNAPII, RNA polymerase II; SRC, sarcoma kinase; SelectFluor, 1-chloromethyl-4-fluoro-1,4-diazoniabicyclo[2.2.2]octane bis(tetrafluoroborate)

■ REFERENCES

(1) Lapenna, S.; Giordano, A. Cell cycle kinases as therapeutic targets for cancer. *Nat. Rev. Drug Discovery* **2009**, *8*, 547−566.

(2) Wang, S.; Fischer, P. M. Cyclin-dependent kinase 9: a key transcriptional regulator and potential drug target in oncology, virology and cardiology. *Trends Pharmacol. Sci.* **2008**, *6*, 302−313.

(3) Cai, D.; Latham, V. M., Jr.; Zhang, X.; Shapiro, G. I. Combined depletion of cell cycle and transcriptional cyclin-dependent kinase activities induces apoptosis in cancer cells. *Cancer Res.* **2006**, *66*, 9270−9280.

(4) Berthet, C.; Aleem, E.; Coppola, V.; Tessarollo, L.; Kaldis, P. Cdk2 knockout mice are viable. *Curr. Biol.* **2003**, *13*, 1775−1785.

(5) Barriere, C.; Santamaria, D.; Cerqueira, A.; Galan, J.; Martin, A.; Ortega, S.; Malumbres, M.; Dubus, P.; Barbacid, M. Mice thrive without Cdk4 and Cdk2. *Mol. Oncol.* **2007**, *1*, 72−83.

(6) Malumbres, M.; Sotillo, R.; Santamaria, D.; Galan, J.; Cerezo, A.; Ortega, S.; Dubus, P.; Barbacid, M. Mammalian cells cycle without the D-type cyclin-dependent kinases Cdk4 and Cdk6. *Cell* **2004**, *118*, 493−504.

(7) Santamaria, D.; Barriere, C.; Cerqueira, A.; Hunt, S.; Tardy, C.; Newton, K.; Caceres, J. F.; Dubus, P.; Malumbres, M.; Barbacid, M. Cdk1 is sufficient to drive the mammalian cell cycle. *Nature* **2007**, *448*, 811−815.

(8) Shapiro, G. I. Cyclin-dependent kinase pathways as targets for cancer treatment. *J. Clin. Oncol.* **2006**, *24*, 1770−1783.

(9) Shiekhattar, R.; Mermelstein, F.; Fisher, R. P.; Drapkin, R.; Dynlacht, B.; Wessling, H. C.; Morgan, D. O.; Reinberg, D. Cdk-activating kinase complex is a component of human transcription factor TFIIH. *Nature* **1995**, *374*, 283−287.

(10) Fisher, R. P. Secrets of a double agent: CDK7 in cell-cycle control and transcription. *J. Cell Sci.* **2005**, *118*, 5171−5180.

(11) Price, D. H. P-TEFb, a cyclin-dependent kinase controlling elongation by RNA polymerase II. *Mol. Cell. Biol.* **2000**, *20*, 2629−1634.

(12) Garriga, J.; Grana, X. Cellular control of gene expression by T-type cyclin/CDK9 complexes. *Gene* **2004**, *337*, 15−23.

(13) Marshall, R. M.; Grana, X. Mechanisms controlling CDK9 activity. *Front. Biosci.* **2006**, *11*, 2598−2613.

(14) Garriga, J.; Bhattacharya, S.; Calbo, J.; Marshall, R. M.; Truongcao, M.; Haines, D. S.; Grana, X. CDK9 is constitutively expressed throughout the cell cycle, and its steady-state expression is independent of SKP2. *Mol. Cell. Biol.* **2003**, *23*, 5165−5173.

(15) Fischer, P. M.; Gianella-Borradori, A. CDK inhibitors in clinical development for the treatment of cancer. *Expert Opin. Invest. Drugs* **2003**, *12*, 955−970.

(16) Byrd, J. C.; Lin, T. S.; Dalton, J. T.; Wu, D.; Phelps, M. A.; Fischer, B.; Moran, M.; Blum, K. A.; Rovin, B.; Brooker-McEldowney, M.; Broering, S.; Schaaf, L. J.; Johnson, A. J.; Lucas, D. M.; Heerema, N. A.; Lozanski, G.; Young, D. C.; Suarez, J. R.; Colevas, A. D.; Grever, M. R. Flavopiridol administered using a pharmacologically derived schedule is associated with marked clinical efficacy in refractory, genetically high-risk chronic lymphocytic leukemia. *Blood* **2007**, *109*, 399−404.

(17) Christian, B. A.; Grever, M. R.; Byrd, J. C.; Lin, T. S. Flavopiridol in chronic lymphocytic leukemia: a concise review. *Clin. Lymphoma Myeloma* **2009**, *9* (Suppl. 3), S179−S185.

(18) Liu, X.; Shi, S.; Lam, F.; Pepper, C.; Fischer, P. M.; Wang, S. CDKI-71, a novel CDK9 inhibitor, is preferentially cytotoxic to cancer cells compared to flavopiridol. *Int. J. Cancer* **2012**, *130*, 1216−1226.

(19) Caracciolo, V.; Laurenti, G.; Romano, G.; Carnevale, V.; Cimini, A. M.; Crozier-Fitzgerald, C.; Gentile, E.; Russo, G.; Giordano, A. Flavopiridol induces phosphorylation of AKT in a human glioblastoma cell line, in contrast to siRNA-mediated silencing of Cdk9: implications for drug design and development. *Cell Cycle* **2012**, *11*, 1202−1216.

(20) Chen, R.; Keating, M. J.; Gandhi, V.; Plunkett, W. Transcription inhibition by flavopiridol: mechanism of chronic lymphocytic leukemia cell death. *Blood* **2005**, *106*, 2513−2519.

(21) Krystof, V.; Baumli, S.; Furst, R. Perspective of cyclin-dependent kinase 9 (CDK9) as a drug target. *Curr. Pharm. Des.* **2012**, *18*, 2883−2890.

(22) Meijer, L.; Raymond, E. Roscovitine and other purines as kinase inhibitors. From starfish oocytes to clinical trials. *Acc. Chem. Res.* **2003**, *36*, 417−425.

(23) Wang, S.; McClue, S. J.; Ferguson, J. R.; Hull, J. D.; Stokes, S.; Parsons, S.; Westwood, R.; Fischer, P. M. Synthesis and configuration of the cyclin-dependent kinase inhibitor roscovitine and its enantiomer. *Tetrahedron: Asymmetry* **2001**, *12*, 2891−2894.

(24) McClue, S. J.; Blake, D.; Clarke, R.; Cowan, A.; Cummings, L.; Fischer, P. M.; MacKenzie, M.; Melville, J.; Stewart, K.; Wang, S.; Zhelev, N.; Zheleva, D.; Lane, D. P. In vitro and in vivo antitumor properties of the cyclin dependent kinase inhibitor CYC202 (*R*-roscovitine). *Int. J. Cancer* **2002**, *102*, 463−468.

(25) Lacrima, K.; Valentini, A.; Lambertini, C.; Taborelli, M.; Rinaldi, A.; Zucca, E.; Catapano, C.; Cavalli, F.; Gianella-Borradori, A.; Maccallum, D. E.; Bertoni, F. In vitro activity of cyclin-dependent kinase inhibitor CYC202 (seliciclib, *R*-roscovitine) in mantle cell lymphomas. *Ann. Oncol.* **2005**, *16*, 1169−1176.

(26) MacCallum, D. E.; Melville, J.; Frame, S.; Watt, K.; Anderson, S.; Gianella-Borradori, A.; Lane, D. P.; Green, S. R. Seliciclib (CYC202, *R*-roscovitine) induces cell death in multiple myeloma cells by inhibition of RNA polymerase II-dependent transcription and down-regulation of Mcl-1. *Cancer Res.* **2005**, *65*, 5399−5407.

(27) Anderson, M.; Andrews, D. M.; Barker, A. J.; Brassington, C. A.; Breed, J.; Byth, K. F.; Culshaw, J. D.; Finlay, M. R.; Fisher, E.; McMiken, H. H.; Green, C. P.; Heaton, D. W.; Nash, I. A.; Newcombe, N. J.; Oakes, S. E.; Pauptit, R. A.; Roberts, A.; Stanway, J. J.; Thomas, A. P.; Tucker, J. A.; Walker, M.; Weir, H. M. Imidazoles: SAR and development of a potent class of cyclin-dependent kinase inhibitors. *Bioorg. Med. Chem. Lett.* **2008**, *18*, 5487−5492.

(28) Chu, X. J.; DePinto, W.; Bartkovitz, D.; So, S. S.; Vu, B. T.; Packman, K.; Lukacs, C.; Ding, Q.; Jiang, N.; Wang, K.; Goelzer, P.; Yin, X.; Smith, M. A.; Higgins, B. X.; Chen, Y.; Xiang, Q.; Moliterni, J.; Kaplan, G.; Graves, B.; Lovey, A.; Fotouhi, N. Discovery of [4-amino-2-(1-methanesulfonylpiperidin-4-ylamino)pyrimidin-5-yl](2,3-difluoro-6-methoxyphenyl)methanone (R547), a potent and selective cyclin-dependent kinase inhibitor with significant in vivo antitumor activity. *J. Med. Chem.* **2006**, *49*, 6549−6560.

(29) DePinto, W.; Chu, X. J.; Yin, X.; Smith, M.; Packman, K.; Goelzer, P.; Lovey, A.; Chen, Y.; Qian, H.; Hamid, R.; Xiang, Q.; Tovar, C.; Blain, R.; Nevins, T.; Higgins, B.; Luistro, L.; Kolinsky, K.; Felix, B.; Hussain, S.; Heimbrook, D. In vitro and in vivo activity of R547: a potent and selective cyclin-dependent kinase inhibitor currently in phase I clinical trials. *Mol. Cancer Ther.* **2006**, *5*, 2644−2658.
(30) Wyatt, P. G.; Woodhead, A. J.; Berdini, V.; Boulstridge, J. A.; Carr, M. G.; Cross, D. M.; Davis, D. J.; Devine, L. A.; Early, T. R.; Feltell, R. E.; Lewis, E. J.; McMenamin, R. L.; Navarro, E. F.; O'Brien, M. A.; O'Reilly, M.; Reule, M.; Saxty, G.; Seavers, L. C.; Smith, D. M.; Squires, M. S.; Trewartha, G.; Walker, M. T.; Woolford, A. J. Identification of *N*-(4-piperidinyl)-4-(2,6-dichlorobenzoylamino)-1*H*-pyrazole-3-carboxamide (AT7519), a novel cyclin dependent kinase inhibitor using fragment-based X-ray crystallography and structure based drug design. *J. Med. Chem.* **2008**, *51*, 4986−4999.
(31) Malumbres, M.; Barbacid, M. Cell cycle, CDKs and cancer: a changing paradigm. *Nat. Rev. Cancer* **2009**, *9*, 153−166.
(32) Wang, S.; Griffiths, G.; Midgley, C. A.; Barnett, A. L.; Cooper, M.; Grabarek, J.; Ingram, L.; Jackson, W.; Kontopidis, G.; McClue, S. J.; McInnes, C.; McLachlan, J.; Meades, C.; Mezna, M.; Stuart, I.; Thomas, M. P.; Zheleva, D. I.; Lane, D. P.; Jackson, R. C.; Glover, D. M.; Blake, D. G.; Fischer, P. M. Discovery and characterization of 2-anilino-4-(thiazol-5-yl)pyrimidine transcriptional CDK inhibitors as anticancer agents. *Chem. Biol.* **2010**, *17*, 1111−1121.
(33) Baumli, S.; Hole, A. J.; Noble, M. E.; Endicott, J. A. The CDK9 C-helix exhibits conformational plasticity that may explain the selectivity of CAN508. *ACS Chem. Biol.* **2012**, *7*, 811−816.
(34) Hole, A. J.; Baumli, S.; Shao, H.; Shi, S.; Huang, S.; Pepper, C.; Fischer, P. M.; Wang, S.; Endicott, J. A.; Noble, M. E. Comparative structural and functional studies of 4-(thiazol-5-yl)-2-(phenylamino)-pyrimidine-5-carbonitrile CDK9 inhibitors suggest the basis for isotype selectivity. *J. Med. Chem.* **2012**, DOI: 10.1021/jm301495v.
(35) Wang, S.; Meades, C.; Wood, G.; Osnowski, A.; Anderson, S.; Yuill, R.; Thomas, M.; Mezna, M.; Jackson, W.; Midgley, C.; Griffiths, G.; Fleming, I.; Green, S.; McNae, I.; Wu, S. Y.; McInnes, C.; Zheleva, D.; Walkinshaw, M. D.; Fischer, P. M. 2-Anilino-4-(thiazol-5-yl)pyrimidine CDK inhibitors: synthesis, SAR analysis, X-ray crystallography, and biological activity. *J. Med. Chem.* **2004**, *47*, 1662−1675.
(36) Nyffeler, P. T.; Duron, S. G.; Burkart, M. D.; Vincent, S. P.; Wong, C. H. SelectFluor: mechanistic insight and applications. *Angew. Chem., Int. Ed.* **2004**, *44*, 192−212.
(37) Finlay, M. R.; Acton, D. G.; Andrews, D. M.; Barker, A. J.; Dennis, M.; Fisher, E.; Graham, M. A.; Green, C. P.; Heaton, D. W.; Karoutchi, G.; Loddick, S. A.; Morgentin, R.; Roberts, A.; Tucker, J. A.; Weir, H. M. Imidazole piperazines: SAR and development of a potent class of cyclin-dependent kinase inhibitors with a novel binding mode. *Bioorg. Med. Chem. Lett.* **2008**, *18*, 4442−4446.
(38) Roshchupkina, G. A.; Pervukhina, N. V.; Rybalova, T. V.; Gatilov, Y. V.; Burdukov, A. B.; Reznikov, V. A. Heterocyclization reaction of alpha-imino carbonyl compounds. Derivatives of 2,5-dihydro-1*H*-imidazole nitroxides. *Eur. J. Org. Chem.* **2003**, *22*, 4432−4437.
(39) Crousier, J.; Metzger, J. Reaction in thiazole series. Action of *N*-butyl lithium on 2-methyl thiazole. *Bull. Soc. Chim. Fr.* **1967**, *11*, 4134−4138.
(40) Shafiee, A.; Hadizadeh, F. Syntheses of substituted pyrrolo[2,3-*d*]imidazoles. *J. Heterocycl. Chem.* **1997**, *34*, 549−550.
(41) Zhang, X. G.; Qing, F. L.; Yu, Y. H. Synthesis of 2′,3′-dideoxy-2′-trifluoromethylnucleosides from alpha-trifluoromethyl-alpha,beta-unsaturated ester. *J. Org. Chem.* **2000**, *65*, 7075−7082.
(42) Nabana, T.; Togo, H. Reactivities of novel [hydroxy(tosyloxy)-iodo]arenes and [hydroxy(phosphoryloxy)iodo]arenes for alpha-tosyloxylation and alpha-phosphoryloxylation of ketones. *J. Org. Chem.* **2002**, *67*, 4362−4365.
(43) Kaila, J. C.; Baraiya, A. B.; Pandya, A. N.; Jalani, H. B.; Vasu, K. K.; Sudarsanam, V. A convenient synthesis of di- and trisubstituted 2-aminoimidazoles from 1-amidino-3-trityl-thioureas. *Tetrahedron Lett.* **2009**, *50*, 3955−3958.
(44) Wang, S.; Wood, G.; Meades, C.; Griffiths, G.; Midgley, C.; McNae, I.; McInnes, C.; Anderson, S.; Jackson, W.; Mezna, M.; Yuill, R.; Walkinshaw, M.; Fischer, P. M. Synthesis and biological activity of 2-anilino-4-(1*H*-pyrrol-3-yl) pyrimidine CDK inhibitors. *Bioorg. Med. Chem. Lett.* **2004**, *14*, 4237−4240.
(45) Endicott, J. A.; Noble, M. E.; Johnson, L. N. The structural basis for control of eukaryotic protein kinases. *Annu. Rev. Biochem.* **2012**, *81*, 587−613.
(46) Cohen, M. S.; Zhang, C.; Shokat, K. M.; Taunton, J. Structural bioinformatics-based design of selective, irreversible kinase inhibitors. *Science* **2005**, *308*, 1318−1321.
(47) Noble, M. E.; Endicott, J. A.; Johnson, L. N. Protein kinase inhibitors: insights into drug design from structure. *Science* **2004**, *303*, 1800−1805.
(48) Davies, T. G.; Bentley, J.; Arris, C. E.; Boyle, F. T.; Curtin, N. J.; Endicott, J. A.; Gibson, A. E.; Golding, B. T.; Griffin, R. J.; Hardcastle, I. R.; Jewsbury, P.; Johnson, L. N.; Mesguiche, V.; Newell, D. R.; Noble, M. E.; Tucker, J. A.; Wang, L.; Whitfield, H. J. Structure-based design of a potent purine-based cyclin-dependent kinase inhibitor. *Nat. Struct. Biol.* **2002**, *9*, 745−749.
(49) Xiao, S.; Raleigh, D. P. A critical assessment of putative gatekeeper interactions in the villin headpiece helical subdomain. *J. Mol. Biol.* **2010**, *401*, 274−285.
(50) Mobilio, D.; Walker, G.; Brooijmans, N.; Nilakantan, R.; Denny, R. A.; Dejoannis, J.; Feyfant, E.; Kowticwar, R. K.; Mankala, J.; Palli, S.; Punyamantula, S.; Tatipally, M.; John, R. K.; Humblet, C. A protein relational database and protein family knowledge bases to facilitate structure-based design analyses. *Chem. Biol. Drug Des.* **2010**, *76*, 142−153.
(51) Baumli, S.; Lolli, G.; Lowe, E. D.; Troiani, S.; Rusconi, L.; Bullock, A. N.; Debreczeni, J. E.; Knapp, S.; Johnson, L. N. The structure of P-TEFb (CDK9/cyclin T1), its complex with flavopiridol and regulation by phosphorylation. *EMBO J.* **2008**, *27*, 1907−1918.
(52) Carlson, B. A.; Dubay, M. M.; Sausville, E. A.; Brizuela, L.; Worland, P. J. Flavopiridol induces G1 arrest with inhibition of cyclin-dependent kinase (CDK) 2 and CDK4 in human breast carcinoma cells. *Cancer Res.* **1996**, *56*, 2973−2978.
(53) Pepper, C.; Lin, T. T.; Pratt, G.; Hewamana, S.; Brennan, P.; Hiller, L.; Hills, R.; Ward, R.; Starczynski, J.; Austen, B.; Hooper, L.; Stankovic, T.; Fegan, C. Mcl-1 expression has in vitro and in vivo significance in chronic lymphocytic leukemia and is associated with other poor prognostic markers. *Blood* **2008**, *112*, 3807−3817.
(54) Awan, F. T.; Kay, N. E.; Davis, M. E.; Wu, W.; Geyer, S. M.; Leung, N.; Jelinek, D. F.; Tschumper, R. C.; Secreto, C. R.; Lin, T. S.; Grever, M. R.; Shanafelt, T. D.; Zent, C. S.; Call, T. G.; Heerema, N. A.; Lozanski, G.; Byrd, J. C.; Lucas, D. M. Mcl-1 expression predicts progression-free survival in chronic lymphocytic leukemia patients treated with pentostatin, cyclophosphamide, and rituximab. *Blood* **2009**, *113*, 535−547.
(55) Nencioni, A.; Hua, F.; Dillon, C. P.; Yokoo, R.; Scheiermann, C.; Cardone, M. H.; Barbieri, E.; Rocco, I.; Garuti, A.; Wesselborg, S.; Belka, C.; Brossart, P.; Patrone, F.; Ballestrero, A. Evidence for a protective role of Mcl-1 in proteasome inhibitor-induced apoptosis. *Blood* **2005**, *105*, 3255−3262.
(56) Veronese, L.; Tournilhac, O.; Verrelle, P.; Davi, F.; Dighiero, G.; Chautard, E.; Veyrat-Masson, R.; Kwiatkowski, F.; Goumy, C.; Vago, P.; Travade, P.; Tchirkov, A. Low MCL-1 mRNA expression correlates with prolonged survival in B-cell chronic lymphocytic leukemia. *Leukemia* **2008**, *22*, 1291−1303.
(57) Brown, N. R.; Noble, M. E.; Lawrie, A. M.; Morris, M. C.; Tunnah, P.; Divita, G.; Johnson, L. N.; Endicott, J. A. Effects of phosphorylation of threonine 160 on cyclin-dependent kinase 2 structure and activity. *J. Biol. Chem.* **1999**, *274*, 8746−8756.
(58) Kabsch, W. XDS. *Acta Crystallogr., Sect. D: Biol. Crystallogr.* **2010**, *66*, 125−132.

(59) Collaborative computational project, number 4. The CCP4 suite: programs for protein crystallography. *Acta Crystallogr.* **1994**, *D50*, 760−763.
(60) Adams, P. D.; Afonine, P. V.; Bunkoczi, G.; Chen, V. B.; Davis, I. W.; Echols, N.; Headd, J. J.; Hung, L. W.; Kapral, G. J.; Grosse-Kunstleve, R. W.; McCoy, A. J.; Moriarty, N. W.; Oeffner, R.; Read, R. J.; Richardson, D. C.; Richardson, J. S.; Terwilliger, T. C.; Zwart, P. H. PHENIX: a comprehensive Python-based system for macromolecular structure solution. *Acta Crystallogr., Sect. D: Biol. Crystallogr.* **2010**, *66*, 213−221.
(61) Murshudov, G. N.; Vagin, A. A.; Dodson, E. J. Refinement of macromolecular structures by the maximum-likelihood method. *Acta Crystallogr., Sect. D: Biol. Crystallogr.* **1997**, *53*, 240−255.
(62) McCoy, A. J.; Grosse-Kunstleve, R. W.; Adams, P. D.; Winn, M. D.; Storoni, L. C.; Read, R. J. Phaser crystallographic software. *J. Appl. Crystallogr.* **2007**, *40*, 658−674.
(63) Emsley, P.; Lohkamp, B.; Scott, W. G.; Cowtan, K. Features and development of Coot. *Acta Crystallogr., Sect. D: Biol. Crystallogr.* **2010**, *66*, 486−501.